AD-A096 720 AIR FORCE GEOPHYSICS LAB HANSCOM AFB MA F/G 16/4.2
SEISMIC HAZARDS STUDIES FOR MINUTEMAN MISSILE WINGS.(U)
SEP 80 J C BATTIS
UNCLASSIFIED AFGL-TR-80-0293 NL

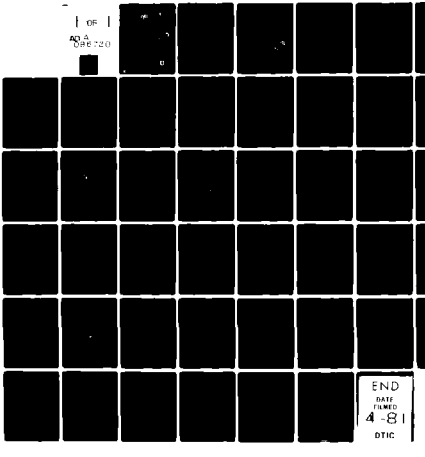

AFGL-TR-80-0293
AIR FORCE SURVEYS IN GEOPHYSICS, NO. 431

LEVEL II

AD A096720

Seismic Hazards Studies for Minuteman Missile Wings.

JAMES C. BATTIS

Final rept.

731

AFGL-TR-80-0293
AFGL-AFSG-431

9 September 1980

DTIC ELECTE MAR 24 1981

Approved for public release; distribution unlimited.

TERRESTRIAL SCIENCES DIVISION PROJECT 7600
AIR FORCE GEOPHYSICS LABORATORY
HANSCOM AFB, MASSACHUSETTS 01731

AIR FORCE SYSTEMS COMMAND, USAF

DTIC FILE COPY

409578

81 3 24 082

This report has been reviewed by the ESD Information Office (OI) and is releasable to the National Technical Information Service (NTIS).

This technical report has been reviewed and is approved for publication.

FOR THE COMMANDER

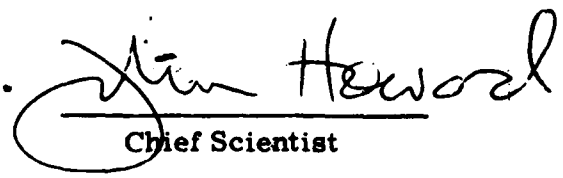

Chief Scientist

Qualified requestors may obtain additional copies from the Defense Documentation Center. All others should apply to the National Technical Information Service.

Unclassified

SECURITY CLASSIFICATION OF THIS PAGE (When Data Entered)

REPORT DOCUMENTATION PAGE		READ INSTRUCTIONS BEFORE COMPLETING FORM
1. REPORT NUMBER AFGL-TR-80-0293	2. GOVT ACCESSION NO. AD-A096720	3. RECIPIENT'S CATALOG NUMBER
4. TITLE (and Subtitle) SEISMIC HAZARDS STUDIES FOR MINUTEMAN MISSILE WINGS		5. TYPE OF REPORT & PERIOD COVERED Scientific. Final. 6. PERFORMING ORG. REPORT NUMBER AFSG No. 431
7. AUTHOR(s) James C. Battis		8. CONTRACT OR GRANT NUMBER(s)
9. PERFORMING ORGANIZATION NAME AND ADDRESS Air Force Geophysics Laboratory (LWH) Hanscom AFB Massachusetts 01731		10. PROGRAM ELEMENT, PROJECT, TASK AREA & WORK UNIT NUMBERS 62101F 76000902
11. CONTROLLING OFFICE NAME AND ADDRESS Air Force Geophysics Laboratory (LWH) Hanscom AFB Massachusetts 01731		12. REPORT DATE 9 September 1980 13. NUMBER OF PAGES 72
14. MONITORING AGENCY NAME & ADDRESS (if different from Controlling Office)		15. SECURITY CLASS. (of this report) Unclassified 15a. DECLASSIFICATION/DOWNGRADING SCHEDULE

16. DISTRIBUTION STATEMENT (of this Report)

Approved for public release; distribution unlimited.

17. DISTRIBUTION STATEMENT (of the abstract entered in Block 20, if different from Report)

18. SUPPLEMENTARY NOTES

19. KEY WORDS (Continue on reverse side if necessary and identify by block number)

Seismic risk
Seismic motion
Earthquake effects
Ground motion attenuation

20. ABSTRACT (Continue on reverse side if necessary and identify by block number)

Using standard methods of probabilistic seismic risk analysis, estimates of the seismic hazards for six Minuteman missile wings were evaluated. The wings are located at Malstrom, Ellsworth, Minot, Whiteman, F. E. Warren and Grand Forks Air Force Bases. For each site, estimates of the site intensity, acceleration, velocity and displacement annual risk curves were made based on the historical seismicity within 1000 km of each site. Based on these curves, composite design response spectra for 10-, 100-, and 1000-year return period motions were calculated. Plots of the reported earthquake

DTIC ELECTE MAR 24 1981 S D C

DD FORM 1 JAN 73 1473

Unclassified

SECURITY CLASSIFICATION OF THIS PAGE When Data Entered

20. (Cont)

epicenters near each site were also generated. To conduct these studies, a new method for regional modification of peak acceleration attenuation functions was developed and is presented in the appendix to this report. Modifications to this scheme are presently being made and are expected to result in some change in the risk estimates for Whiteman AFB.

Accession For
NTIS GRA&I
DTIC TAB
Unannounced
Justification
By
Distribution/
Availability Codes
Dist | Avail and/or Special
A

Contents

Illustrations

Illustrations

Tables

Tables

Seismic Hazards Studies for Minuteman Missile Wings

1. INTRODUCTION

On 28 March 1975, an earthquake of magnitude 6.1 m_b occurred in the Pocatello Valley of southeastern Idaho. Although located nearly 700 km east of the earthquake epicenter and well outside of the limits of the felt area for this event, the 90th Strategic Missile Wing, located at F. E. Warren AFB, experienced significant operational status changes as a result of the seismic motions generated by this event. This situation indicated the need for an examination of the seismic hazard for each of the Minuteman Missile Wings. This report discusses the seismic hazard evaluations conducted for the six Minuteman Wings located at Malstrom, Ellsworth, Minot, Whiteman, F. E. Warren and Grand Forks Air Force Bases (Figure 1). For each of these facilities, annual risk curves for intensity and peak acceleration, velocity, and displacement are presented. The uncertainties which effect these evaluations are discussed and horizontal design response spectra based on these curves are given. Finally, a brief discussion of the local seismic history for each wing is presented.

(Received for publication 9 September 1980)

PRECEDING PAGE BLANK-NOT FILMED

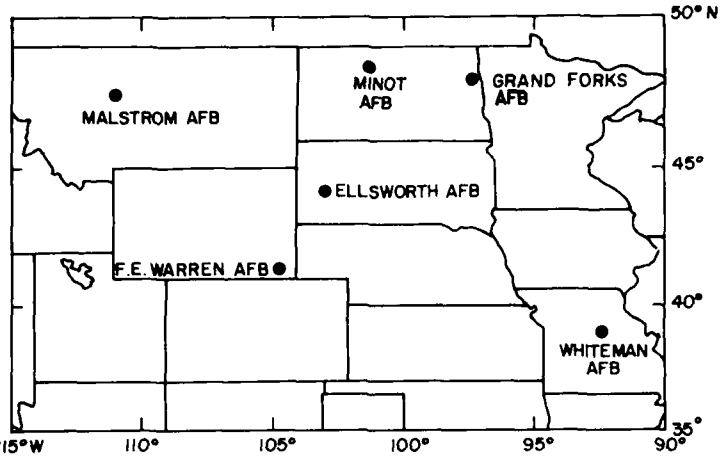

Figure 1. Map of the North Central United States Showing the Location of the Six Minuteman Wings Studied in This Report

2. SEISMIC HAZARD ANALYSIS

2.1 Seismic Hazard Estimation

Seismic hazard analysis can be approached in two ways; using either deterministic or probabilistic methods. Deterministic analysis relies on the detailed knowledge of earthquake faults in the vicinity of site of interest. For each fault, a maximum credible earthquake is estimated and the resulting ground motions at the site of interest, using conservative assumptions, are estimated for each of these events. This method provides an upper bound estimate for the ground motion at the site of interest with no consideration of the frequency of occurrence. The probabilistic approach uses the historical seismicity in the vicinity of the site to generate statistical estimates of future activity. Probabilistic estimates of ground motion at the site can then be calculated from this information. The deterministic approach requires geologic field studies which are typically not available for the regions examined in this report. For this reason only the probabilistic procedure was applied in the evaluation of seismic hazards for the missile wings.

2.2 Seismicity Studies

The first step in the determination of probabilistic hazard estimates is the development of a statistical model of the seismic activity in a region around the site of interest. Using historical earthquake data, areas of concentrated seismic

activity or common tectonic setting, known as seismic source regions, are identified and delineated. All activity outside of these regions is treated as a unit called the background activity. As there is no geophysical basis for limiting the location of the background activity, these events are assumed to occur with equal probability throughout the area with the exception of the specified source regions.

It should be noted that the lack of sufficient geological studies, imprecise epicenter location, and incomplete earthquake reporting make the boundaries of all source regions somewhat arbitrary. For source regions at large distances from the site of interest, the effects of this uncertainty are negligible. As the site-to-source distance becomes small, however, this problem can introduce significant variability into the seismic hazard estimation.

For each of the defined source zones and the background, estimates of the level of seismic activity were made by fitting the standard recurrence function[1]

$$\log (N) = A - bM \qquad (1)$$

where

N = the number of events per year of magnitude M or greater,

and

A and b = the regression parameters.

Prior to evaluation of the recurrence curve parameters, the earthquake catalogue for each source region was evaluated for temporal stability using a method developed by Stepp.[2] Where required to obtain stability, appropriate procedures were applied to the earthquake catalogues. These involved the editing of the data over selected time windows for different magnitude ranges to produce stable estimates of recurrence periods within each magnitude range.

The uncertainties associated with the seismicity study are impossible to determine. While the standard error of fitting for the parameters of Eq. (1) to the data can be determined easily, this is only one source of potential error. Studies of the seismicity of regions with long historic earthquake records, such as China and

1. Richter, C. (1958) Elementary Seismology, W. H. Freeman and Co., San Francisco, CA.

2. Stepp, J. (1972) Analysis of completeness of the earthquake sample in the Puget Sound area and its effect on statistical estimates of earthquake hazards, Proceedings of the International Conference on Microzonation for Safer Construction Research and Application, Seattle, WA.

the Middle East, indicate that the relatively short historic record in the United States is probably not adequate to provide a complete description of the seismic activity.[3,4] These studies have shown that the level and location of seismic activity can vary over periods longer than that of the historic record in North America. Apparently inactive faults can return to activity and active regions become quiescent. One prominent example of the former case is the San Fernando Earthquake of 1971 which occurred on a fault which appeared to be inactive. The uncertainty associated with this condition is indeterminant but could be expected to affect both the source regions bounds and recurrence curves used in the risk analysis.

A maximum magnitude earthquake for each source region was also evaluated as part of the seismicity studies. The magnitude of this event was typically determined by adding 0.5 magnitude units to the largest event recorded within the source area and then rounding up to the next higher integral or half magnitude value. This value was used as the upper limit earthquake in the probability calculations. While the method is arbitrary, it is not usually critical to the final risk estimation because the inter-occurrence periods of these events are typically much longer than the lowest level of risk examined, and contribute only slightly to the estimation of ground motion at the site of interest.

For each base examined in this report, the seismic activity within 1000 km of the site was used in the seismicity study. The source of the historical earthquake data was the National Oceanic and Atmospheric Administration Earthquake Data File.[5] This file covers earthquake activity in the United States from 1683 to 1978 but with varying degrees of completeness. Prior to 1899 this listing is restricted to earthquakes of epicentral intensity V or greater. For earthquakes of magnitudes 5.0 m_b or greater, completeness is reached in the early 20th century for the areas studied in this report. Apparent stability exists for the range of 4.0 to 5.0 m_b in the early 1960's with the advent of the World Wide Standard Seismograph Network (WWSSN). In general, seismic activity below magnitude 4.0 m_b is reported only erratically. The accuracy of epicenter determinations is several tenths of a degree in most cases.

---

3. McGuire, R. (1979) Adequacy of simple probability models for calculating felt shaking hazard using the Chinese earthquake catalog, Bull. Seism. Soc. Am. 69:877-892.
4. Quittmeyer, R., and Jacob, K. (1979) Historical and modern seismicity of south-central Asia, Bull. Seism. Soc. Am. 69:773-823.
5. Meyers, H., and von Hake, C. (1976) Earthquake Data File Summary, National Geophysical and Solar-Terrestrial Data Center Report KGRD-5.

2.3 Ground Motion Attenuation

To relate the temporal and spatial properties of seismic activity to ground motion at the site of interest, it is necessary to have a means of predicting ground motion at the site as a function of earthquake magnitude and epicentral distance. Numerous empirical ground motion attenuation functions have been developed for this purpose. A typical equation has the functional form:

$$\ln g_s = a_1 + a_2 M - a_3 \ln (R + R_o) \qquad (2)$$

where

g_s = the site ground motion,
M = causative event magnitude,
R = epicentral distance,
R_o = a distance factor commonly set to zero or 25 km,

and

a_1, a_2, a_3 = empirically derived constants.

The ground motion descriptor, g_s, is usually peak site acceleration, velocity, or displacement; though other parameters have been used.

Virtually all of the available attenuation functions have one significant deficiency. They have been derived on the basis of data primarily from Southern California earthquakes. The ground motion attenuation in this region is not thought to be typical of the rest of the United States. For this reason, these equations can not be applied blindly outside of California.

To overcome this problem, two different paths were followed to obtain ground motion estimates at the various wings. The first of these was to use Modified Mercalli intensity (Table 1) as the ground motion descriptor. As attenuation curves for intensity can be derived on the basis of historical, non-instrumental earthquake records, they are generally available for all of the United States. The difficulty with this approach is the subsequent conversion from intensity to ground motion descriptors of engineering significance. As the intensity scale was based on subjective and coarse gradations, wide ranges of acceleration, velocity, and displacement have been observed for each intensity level[6] (Figure 2). The conversion from site

6. Trifunac, M., and Brady, A. (1975) On the correlation of seismic intensity scales with peaks of recorded strong ground motion, Bull. Seism. Soc. Am. 65:139-162.

intensity to peak acceleration, velocity, and displacement were made using the relationships derived by Trifunac and Brady.[6] Specifically:

$$\log A_H = -0.014 + 0.30 I_{mm} , \tag{3}$$

$$\log V_H = -0.63 + 0.25 I_{mm} , \tag{4}$$

and

$$\log D_H = -1.13 + 0.24 I_{mm} , \tag{5}$$

where

A_H, V_H, D_H = peak horizontal acceleration, velocity, and displacement respectively, and

I_{mm} = the site Modified Mercalli intensity.

These relations were explicitly derived over the range of intensities from IV to X but have been assumed to apply over the full twelve-point range of the scale for the purposes of this report. It should also be noted that the use of other empirical relations can produce different ground motion levels.

The second approach that was used to develop the seismic risk estimates was to attempt to derive regionally modified peak ground motion attenuation functions for the areas being studied. Only for acceleration was this procedure successful. A description of the method used for regional modification of peak acceleration attenuation functions is given in Appendix A. The results of this analysis indicate that only in the case of Wing IV, Whiteman AFB, Missouri, is the regional attenuation so different from that in California as to require an attenuation function other than an empirical, California data based equation. Since the completion of this study, several useful suggestions to improve the modification scheme of Appendix A have been received (Nuttli, personal communication, 1980). The principal effect of these changes would be to alter the near-field acceleration estimates for the Central United States attenuation function. The hazard estimates at all of the sites except Whiteman AFB are not expected to be affected. Preliminary results suggest a reduction of the estimated seismic risk at Whiteman AFB, however, the degree of change is uncertain. At the present time, the modifications are being incorporated into the technique and a new Central United States attenuation function evaluated. After this has been completed the seismic hazard at Whiteman AFB will be re-evaluated and, if significant changes result, the new risk estimate will be presented at a later date.

Table 1. Modified Mercalli Intensity Scale of 1931

I. Not felt except by a very few under specially-variable circumstances. (I Rosse-Forel scale.)	VIII. Damage slight in specially designated structures; considerable in ordinary substantial buildings with partial collapse; great in poorly built structures. Panel walls thrown out of frame structures. Fall of chimneys, factory stacks, columns, monuments, walls. Heavy furniture overturned. Sand and mud ejected in small amounts. Changes in well water. Persons driving motorcars disturbed. (VIII+ to IX- Rossi-Forel scale.)
II. Felt only by a few persons at rest, especially on upper floors of buildings. Delicately suspended objects may swing. (I to II Rossi-Forel scale.)	IX. Damage considerable in specially designed structures; well-designed frame structures thrown out of plumb; great in substantial buildings, with partial collapse. Buildings shifted off foundations. Ground cracked conspicuously. Underground pipes broken. (IX+ Rossi-Forel scale.)
III. Felt quite noticeably indoors, especially on upper floors of buildings, but many people do not recognize it as an earthquake. Standing motorcars may rock slightly. Duration estimates. (III Rossi-Forel scale.)	X. Some well-built wooden structures destroyed; most masonry and frame structures destroyed with foundations, ground badly cracked. Rails bent. Landslides considerable from riverbanks and steep slopes. Shifted sand and mud. Water splashed (slopped) over banks. (X Rossi-Forel scale.)
IV. During the day felt indoors by many, outdoors by few. At night some awakened. Dishes, windows, doors disturbed; walls make creaking sound. Sensation like heavy truck striking building. Standing motorcars rocked noticeably. (IV to V Rossi-Forel scale.)	XI. Few, if any, (masonry) structures remain standing. Bridges destroyed. Broad fissures in ground. Underground pipelines completely out of service. Earth slumps and land slips in soft ground. Rails bent greatly.
V. Felt by nearly everyone, many awakened. Some dishes, windows, etc., broken; a few instances of cracked plaster; unstable objects overturned. Disturbance of trees, poles, and other tall objects sometimes noticed. Pendulum clocks may stop. (V to VI Rossi-Forel scale.)	XII. Damage total. Waves seen on ground surfaces. Lines of sight and level distorted. Objects thrown upward into air.
VI. Felt by all, many frightened and run outdoors. Some heavy furniture moved; a few instances of fallen plaster or damaged chimneys. Damage slight. (VI to VII Rossi-Forel scale.)	
VII. Everybody runs outdoors. Damage negligible in buildings of good design and construction; slight to moderate in well-built ordinary structures; considerable in poorly built or badly designed structures; some chimneys broken. Noticed by persons driving motorcars. (VIII Rossi-Forel scale.)	

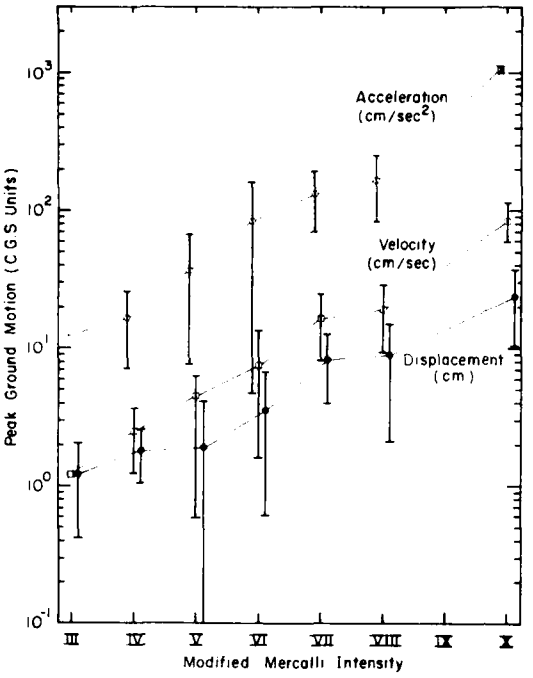

Figure 2. Mean and One Standard Deviation Error Bars Peak Ground Motions Plotted Against Modified Mercalli Intensity at the Observation Site. Acceleration, open circles; velocity, open squares; displacement, solid circles

If the analysis of Appendix A is correct, however, it would appear that most empirically derived functions, being based predominantly on data from less than 100 km, over-estimate far-field accelerations. In Figure 3, the predicted peak accelerations for a magnitude 6.0 earthquake in California have been plotted using the attenuation functions derived in Appendix A and seven empirical functions listed by McGuire.[7] The discrepency at distances greater than about 100 km is apparent. This problem is significant in that for most sites studied in this report, the seismic source regions tend to be at distances greater than 100 km. In turn, one must also be skeptical of the velocity and displacement relations for the same reason. The set of velocity and displacement attenuation functions which predict the lowest mean values at large epicentral distances were those developed by Orphal and Lahoud.[8] These equations were used for risk estimation at all wings except Wing IV. The constants of all ground motion attenuation functions used in this report are given in Table 2.

7. McGuire, R. (1976) FORTRAN Computer Program for Seismic Risk Analysis, U.S. Geol. Surv. Open-File Report 76-67.

8. Orphal, D., and Lahoud, J. (1974) Prediction of peak ground motion from earthquakes, Bull. Seism. Soc. Am. 64:1563-1574.

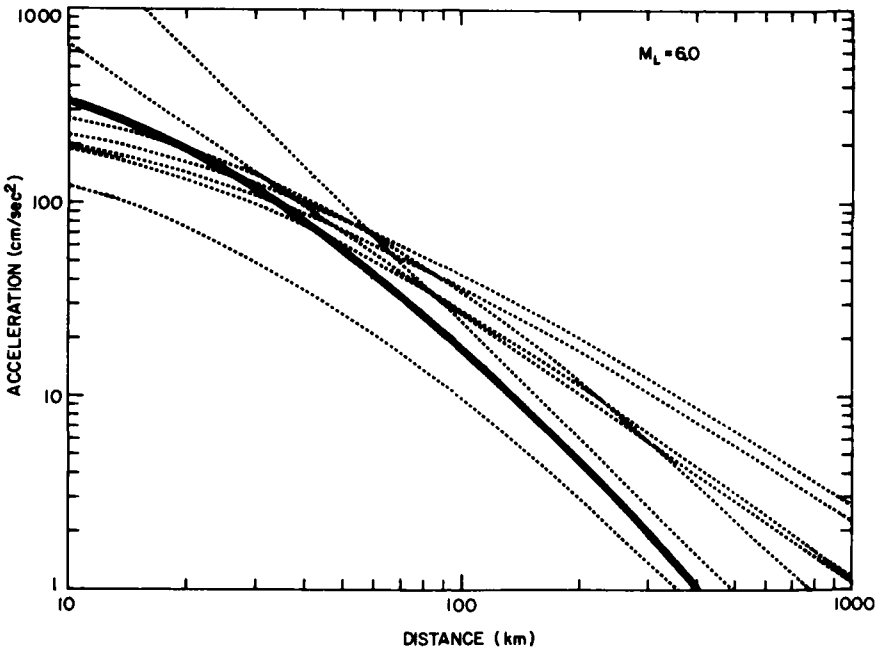

Figure 3. Plot of Peak Ground Acceleration vs Distances for a Magnitude 6.0 M_L Earthquake in Southern California as Predicted by Seven Empirical Curves (dashed lines) and the Derived Curved (solid line) Based on the Analysis of Appendix A

Table 2. Ground Motion Attenuation Functions

Ground Motion	Application	Source	$\ln g_s = \alpha_1 + \alpha_2 M - \alpha_3 \ln(R + R_o)$				
			α_1	α_2	α_3	R_o	$\sigma_{\ln g_s}$
Intensity†	I, II, III, V, VI	Howell and Schultz[7]	2.29	1.42	1.36	0.0	0.68
Intensity†	IV	Howell and Schultz[7]	1.20	2.23	1.36	0.0	0.68
Acceleration	I, II, III, V, VI	Appendix A	8.76	0.812	2.327	25.0	(0.707)*
Acceleration	IV	Appendix A	4.21	1.40	1.57	25.0	(0.707)*
Velocity	I, II, III, V, VI	Orphal and Lahoud[6]	-0.32	1.20	1.34	0.0	(0.707)*
Displacement	I, II, III, V, VI	Orphal and Lahoud[6]	-3.06	1.312	1.18	0.0	(0.760)*

†Conversion from I_o to M using relationships by Brazee[8]

*Assumed value.

2.4 Seismic Risk Estimation

Using a method proposed by Cornell[9] and implemented in a FORTRAN computer program by McGuire[7] the temporal and spatial distribution of seismic activity and the ground motion attenuation functions can be combined into a single statement of the probability of attaining a given level of ground motion at the site of interest. In this procedure, the probability that the ground motion level will reach or exceed a specified level, m_g, is defined as the integral of the product of the independent probability density functions for magnitude, f_S, distance, f_R, and distance, r. This can be stated as an equation:

$$P[M_g \geq m_g] = \int\int P[M_g \geq m_g \mid s \text{ and } r]\, f_S(s)\, f_R(r)\, ds\, dr \qquad (6)$$

where

$P[M_g \geq m_g \mid s \text{ and } r]$ is the condition probability given event magnitude and distance.

The conditional probability of Eq. (6) is a function of the ground motion attenuation equation and its standard deviation. The function $f_S(s)$ is derived from each source region recurrence curve while $f_h(r)$ incorporates the spatial relationship between source region and site of interest. Evaluation of the integral yields the probability of one event from the specified source region reaching or exceeding m_g. By multiplying this value by the expected number of events in the region and accumulating over all source areas, the total expected number of events meeting the conditions, $E[M_g \geq m_g]$, is obtained. Assuming earthquake occurrence is a Poisson process, the annual risk is given by

$$R[M_g \geq m_g] = 1 - e^{-E[M_g \geq m_g]}. \qquad (7)$$

Annual risks can be converted to risks for any given lifetime by the equation:

$$R_N = 1 - (1 - R_A)^N \qquad (8)$$

where

N is the lifetime in years

R_A is the annual risk,

and

R_N is the N-year lifetime risk.

One final term used in describing risk is the return period which is the reciprocal of the risk and describes the number of lifetime periods, on the average, between recurrence of the associated level of ground motion.

2.5 Response Spectra

For engineering purposes, the spectral characteristics of ground motion are typically presented in the form of response spectra. These spectra represent the maximum response of a simple, viscous-damped harmonic oscillator over a range of natural periods for a specified percentage of critical damping. Methods have been developed to estimate upper limit response spectra given the level of ground motion at the site of interest, known as design response spectra.[10] The AEC amplifications factors, given in Table 3, are used to modify the predicted ground motion levels at a site to obtain the response spectra levels at the specified frequencies. These factors give the mean plus one standard deviation response spectra.

Table 3. Horizontal Design Response Spectra Amplification Factors

Critical Damping (%)	Acceleration			Displacement (cm)
	33 Hz	9 Hz	2.5 Hz	0.25 Hz
0.5	1.0	4.96	5.95	3.20
2.0	1.0	3.54	4.25	2.50
5.0	1.0	2.61	3.13	2.05
7.0	1.0	2.27	2.72	1.88
10.0	1.0	1.90	2.28	1.70

The levels of critical damping correspond to soil conditions at the site with lower values associated with harder rock. Most foundation conditions lie between 2.0 and 7.0 percent of critical damping. The lowest damping is always the higher amplitude spectrum. In all response spectra plots in this report the complete

10. Hays, W., Algermissen, S., Estinesa, A., Perkins, D., and Rinehart, W. (1975) Guidelines for Developing Design Earthquake Response Spectra, U.S. Geol. Surv. Technical Report M-114.

range of damping factors given in Table 3 are plotted. Thus, the upper plot is always 0.5 percent and the lower 10 percent of critical damping.

It should be noted that when the design spectra is calculated on the basis of independently evaluated acceleration and displacement levels corresponding to a specified risk level, they are not necessarily a spectral limit for any one earthquake. This is because the ground motions on which they are based may be generated by different earthquakes.[11] In this case, it is more accurate to view the spectra as upper limits for separate frequency bands than as the upper limit spectra for any one earthquake. The spectra, in this case, will be designated as composite response spectra.

3. SEISMIC HAZARD EVALUATIONS

3.1 Malstrom AFB – Wing I

Malstrom AFB is located near one of the most seismically active regions of the continental United States, an area known as the Intermountain Seismic Belt. This zone runs along the northern Rocky Mountains in western Montana through Yellowstone National Park and along the Wasatch Front in Utah. The location of Malstrom AFB relative to these active regions, as shown in Figure 4, suggests a high level of seismic hazard at this facility.

For the purposes of this study, the Intermountain Seismic Belt has been divided into three subregions, Montana, Yellowstone and Utah, to compensate for the variations of seismic activity throughout the zone. In addition, several other source regions were defined by analysis of epicentral clustering and tectonic setting of all earthquakes within 1000 km of Malstrom AFB. These source regions are depicted in Figure 4. The area, recurrence curve constants and maximum magnitude earthquakes for each source region are given in Table 4 along with the background seismicity parameters. The background recurrence curve is assumed to hold in all areas *not* explicitly in a seismic source zone. Thus, while the probability of an earthquake occurring outside of a defined source is low, it is assumed that activity can occur anywhere within 1000 km of the site of interest including areas with no known historical reports of activity. The site used to represent Malstrom AFB in the risk calculations was 47.5°N and 111.0°W.

11. Battis, J. (1978a) Geophysical Studies for Missile Basing Seismic Risk Studies in the Western United States, Texas Instruments Inc., Scientific Report No. 2 ALEX(02)-ISR-78-01.

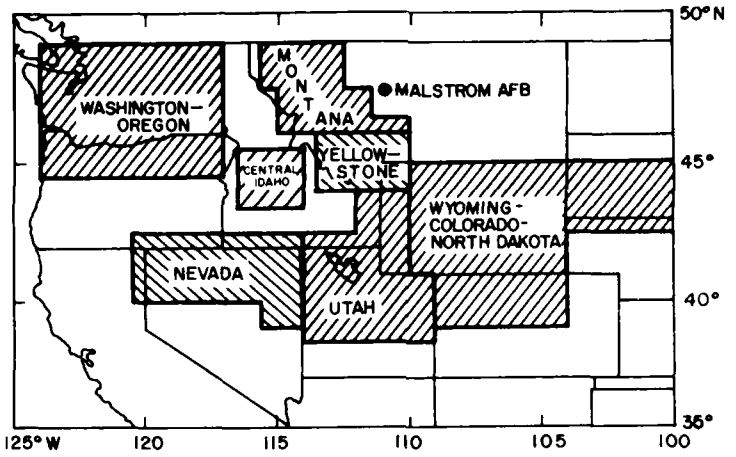

Figure 4. Seismic Source Regions Used to Evaluate the Seismic Hazard at Malstrom AFB (indicated by solid circle)

Table 4. Malstrom AFB Source Region Parameters

Source	Area (10^4 km^2)	log (N/y) = A – bM_L		M_L MAX
		A	B	
Wyoming - Colorado - South Dakota	43.05	2.869	0.592	7.0
Nevada	16.66	4.541	1.031	7.0
Washington - Oregon	26.66	2.806	0.597	7.0
Central Idaho	4.41	3.177	0.792	7.0
Yellowstone	6.11	3.652	0.765	7.0
Montana	7.70	3.101	0.682	7.0
Utah	20.05	3.236	0.690	7.0
Background	-----	2.636†	0.748	6.0

†log (N/y/10^4 km^2)

The estimated annual risk curve for Modified Mercalli intensity is shown in Figure 5 and the peak acceleration, velocity, and displacement curves are displayed in Figure 6. The ground motion levels at specified annual risks are also tabulated in Table 5. In Table 6 the ground motion levels based on the conversion of Modified Mercalli intensity are given. Considering the large standard errors associated

with the conversion of site intensity to the peak ground motion levels, the values in these tables are believed to be in good agreement.

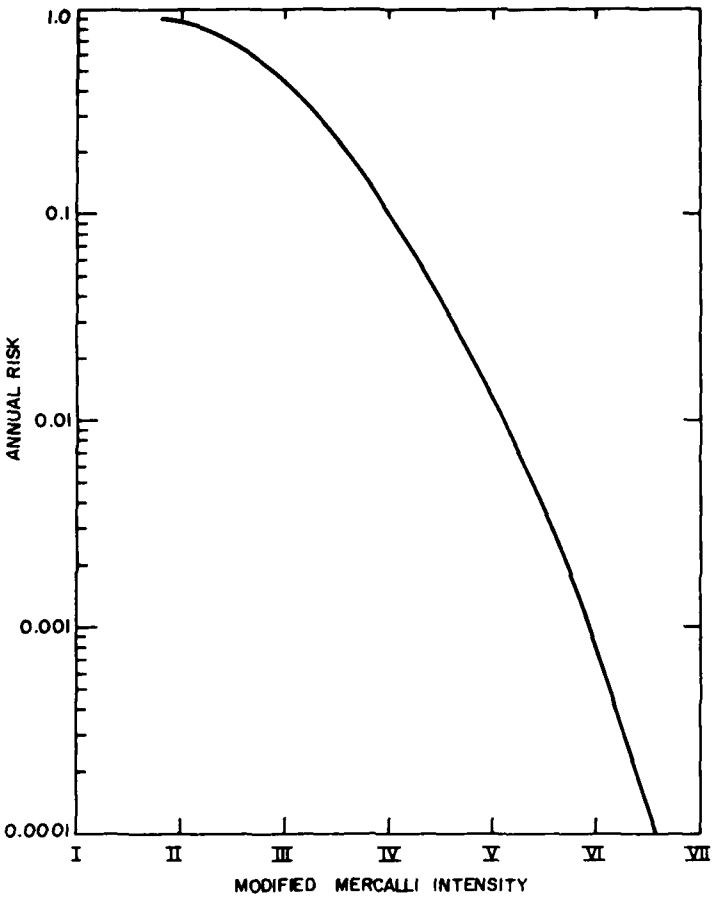

Figure 5. Modified Mercalli Intensity Seismic Risk Curve for Malstrom AFB

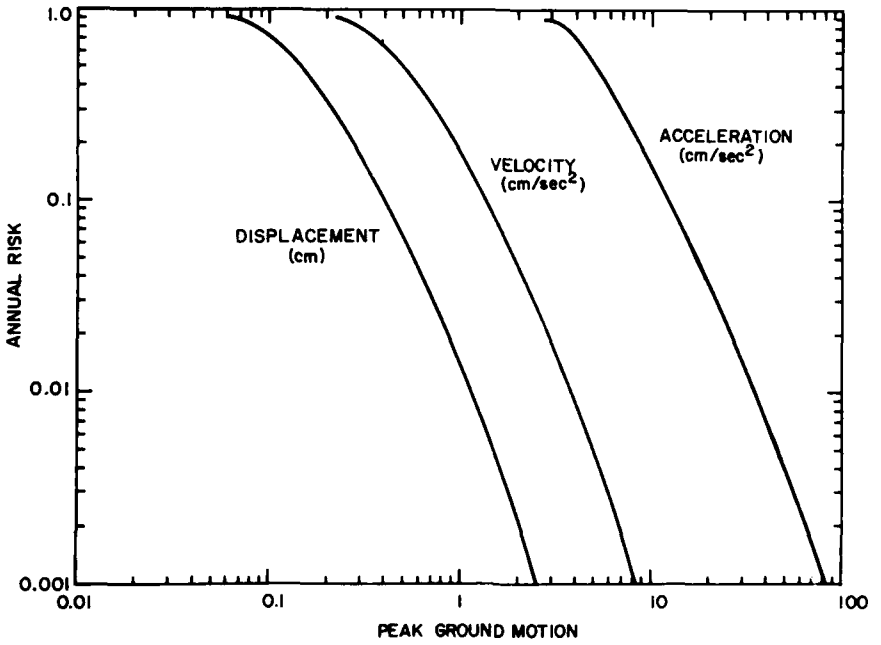

Figure 6. Peak Ground Acceleration, Velocity, and Displacement, Seismic Risk Curves for Malstrom AFB

Table 5. Peak Ground Motion Annual Risk Levels for Malstrom AFB

Annual Risk	Return Period (years)	Intensity	Acceleration (cm/sec^2)	Velocity (cm/sec)	Displacement (cm)
0.9	1.11	II	2.7	0.22	0.06
0.5	2	III	5.1	0.48	0.14
0.2	5	III-IV	8.7	0.91	0.27
0.1	10	IV	12.3	1.34	0.40
0.05	20	IV	17.0	1.87	0.57
0.02	50	IV-V	25.4	2.80	0.86
0.01	100	V	34.1	3.69	1.13
0.005	200	V	45.4	4.79	1.46
0.002	500	V-VI	65.4	6.61	2.00
0.001	1000	VI	85.5	8.33	2.50

Table 6. Peak Ground Motion Annual Risk Levels for Malstrom AFB Based on Intensity Levels

Annual Risk	Fractional Intensity	Acceleration (cm/sec^2)	Velocity (cm/sec)	Displacement (cm)
0.9	1.8	3.5	0.7	0.2
0.5	2.9	6.9	1.2	0.4
0.2	3.6	11.6	1.9	0.5
0.1	4.0	15.3	2.3	0.7
0.05	4.4	19.5	2.9	0.8
0.02	4.8	26.7	3.7	1.1
0.01	5.1	32.8	4.4	1.2
0.005	5.4	39.8	5.1	1.5
0.002	5.7	49.6	6.2	1.7
0.001	5.9	57.8	7.1	2.0

The proximity of the Montana source region to the site of interest, as shown in Figure 4, suggests that a strong spatial gradient of the seismic hazard should be observed in the vicinity of Malstrom AFB. This, in fact, is the case with sharply increasing ground motions at each level of risk observed toward the southwest of the facility. In Figure 7, the peak ground accelerations for an annual risk of 0.002, or return period of 500 years, are contoured over a one-degree square centered on Malstrom AFB. For other levels of risk the contours follow in the same trend. The same characteristics are observed for peak velocity and displacement although the gradient is less severe than for acceleration.

It should be noted that the contour locations are defined by the location of the Montana source region boundaries. Inside of the boundary, neglecting the effects of other source regions, the seismic hazard is uniform. As the boundary is approached what could be termed an edge effect begins to reduce the hazard. Moving away from the source the hazard decreases gradually to a uniform level determined by the background activity. Moving the source region boundary towards the site of interest will increase the seismic hazard at the site and, conversely, moving the boundary away from the site will reduce the hazard. The source region boundaries are somewhat arbitrary due to a lack of detailed fault maps of a complete understanding of the geologic setting associated with earthquakes in this region. For sites near source regions, this can produce a decrease in the level of confidence associated with the estimated ground motion values.

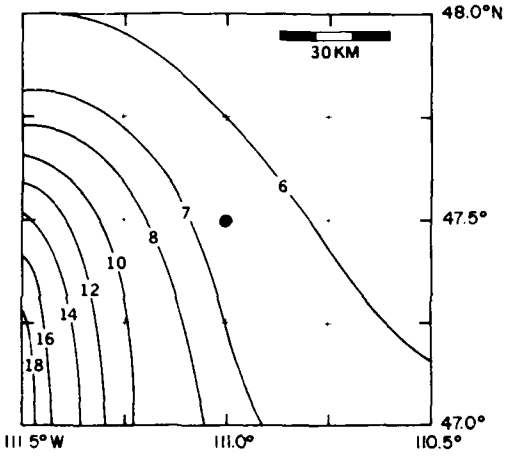

Figure 7. Contours of 500-year Return Period Accelerations in a One-degree Square Centered on Malstrom AFB. (Solid circle); (units in % g)

In Figures 8a, 8b, and 8c the composite horizontal design response spectra for 10-, 100-, and 1000-year return period ground motions, based on the values given in Table 5, are displayed.

In Figure 9, 95 earthquakes between 1972 and 1978 reported in the Earthquake Data File within 200 km of Malstrom AFB are plotted. The closest center of major activity to the site is 120 km to the southwest near Helena, Montana although an earthquake with no recorded magnitude or intensity was reported within 75 km of the base. The largest event reported in this particular area was a magnitude 6.25 M_L event which occurred on 19 October 1935 and is one of the largest earthquakes reported in the northern extent of the Intermountain Seismic Belt. This earthquake was one of a series of events occurring in late 1935 of which four events, including the magnitude 6.25 M_L earthquake, had epicentral intensities of between VI and VIII. At the 90 percent confidence level the predicted ground motions at Malstrom AFB for this event are 21.9 cm/sec^2, 5.1 cm/sec and 1.5 cm/sec. The horizontal design response spectra for this event is shown in Figure 10. An average site intensity determined from these values, Modified Mercalli Intensity V, agrees with the intensity level observed in the vicinity of Great Falls, Montana.[12]

---

12. Neumann, F. (1937) United States Earthquakes, 1935. Department of Commerce, Coast and Geodetic Survey, Serial No. 600.

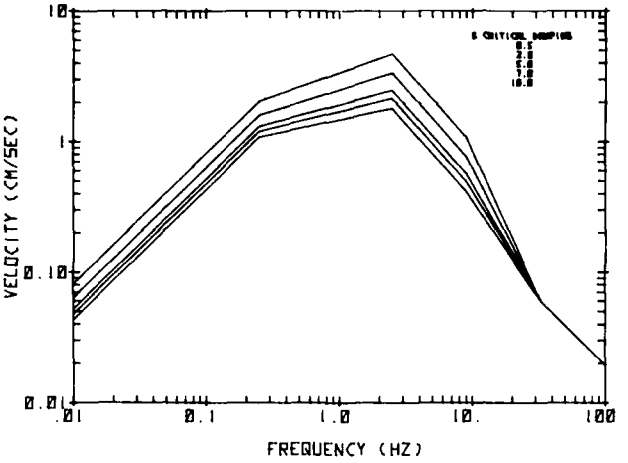

Figure 8a. Composite Horizontal Design Response Spectra for Malstrom AFB Based on 10-year Return Period Ground Motions

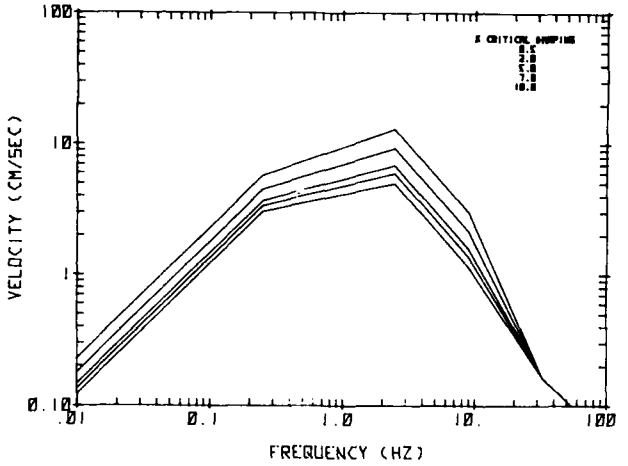

Figure 8b. Composite Horizontal Design Response Spectra for Malstrom AFB Based on 100-year Return Period Ground Motions

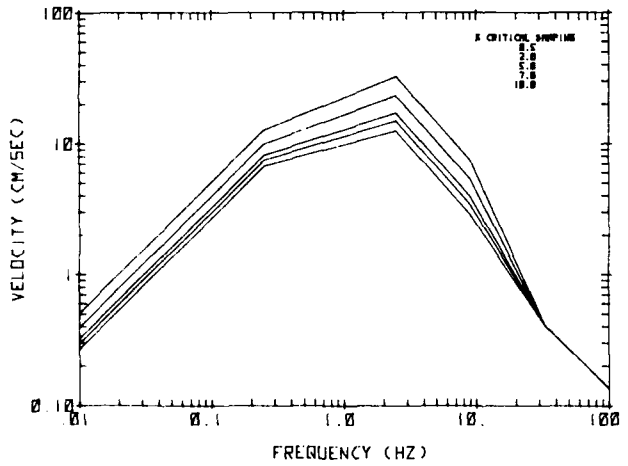

Figure 8c. Composite Horizontal Design Response Spectra for Malstrom AFB Based on 1000-year Return Period Ground Motions

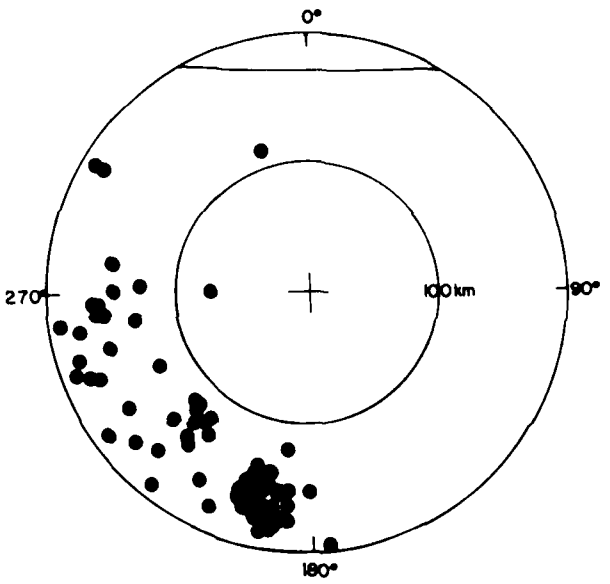

Figure 9. Reported Earthquake Epicenters Within 200 km of Malstrom AFB

At a greater epicentral distance, 170 km, an even larger earthquake, magnitude 6.75 m, was reported on 28 June 1925. The 90 percent confidence ground motions at the site of interest are estimated at 17.2 cm/sec^2, 6.0 cm/sec, and 2.0 cm. The lower acceleration and higher velocity and displacement as compared to the Helena, Montana Earthquake are explained by the longer travel path and the resulting greater attenuation of the high frequency components of the signal. Again, the predicted site intensity of this event at Great Falls, Montana is intensity V. The horizontal design response spectra are shown in Figure 11. The higher amplitudes at low frequency than for the Helena event are the significant feature of this event.

3.2 Ellsworth AFB – Wing II

In Figure 12, the seismic source regions used in the hazard evaluation for Ellsworth AFB are shown and the associated source parameters are given in Table 7. Several of the source regions have been redefined as compared to those used in the previous section. This results from the change in the earthquakes included in the seismicity studies due to the 1000 km radius search limit from the site of interest. In addition, as a result of the greater influence on seismic hazard

by near site source regions, greater care was used in defining the Colorado and Wyoming area source regions. The point used in all calculations for Ellsworth AFB was 44.2°N and 103.0°W.

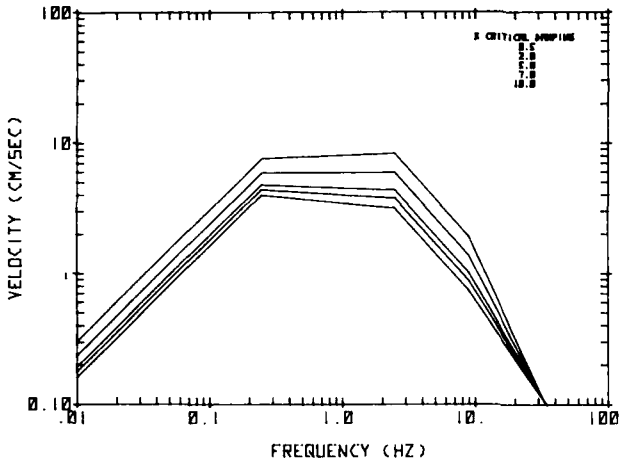

Figure 10. Horizontal Design Response Spectra for Malstrom AFB Assuming a Recurrence of the 1935 Helena, Montana Earthquake (6.25 M_L)

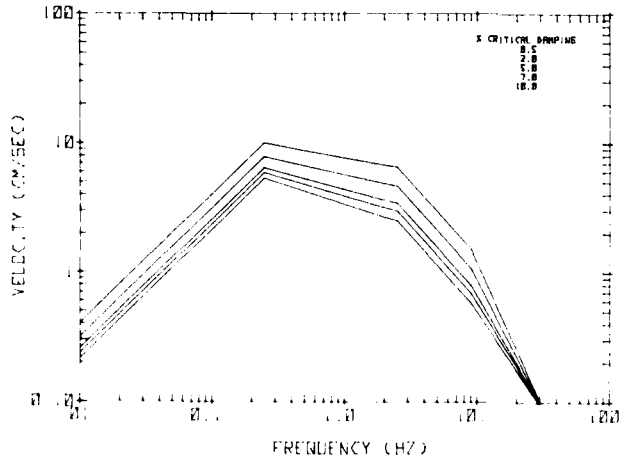

Figure 11. Horizontal Design Response Spectra for Malstrom AFB Assuming a Recurrence of the 1925 Earthquake (6.75 M_L)

Table 7. Ellsworth AFB Source Region Parameters

Source	Area (10^4 km^2)	$\log (N/y) = A - b M_L$		M_L MAX
		A	b	
Central Idaho	4.41	3.177	0.792	7.0
Montana	7.70	3.101	0.682	7.0
Yellowstone	6.11	3.652	0.765	7.0
Colorado	15.83	3.419	0.700	7.0
Wyoming	18.05	4.465	1.114	6.0
Utah	26.19	3.598	0.702	7.5
Nevada	7.58	1.662	0.516	7.0
New Mexico - Texas	9.15	2.574	0.683	7.5
Background	——	1.721†	0.199	6.0

†$\log(N/y, 10^4 \text{ km}^2)$

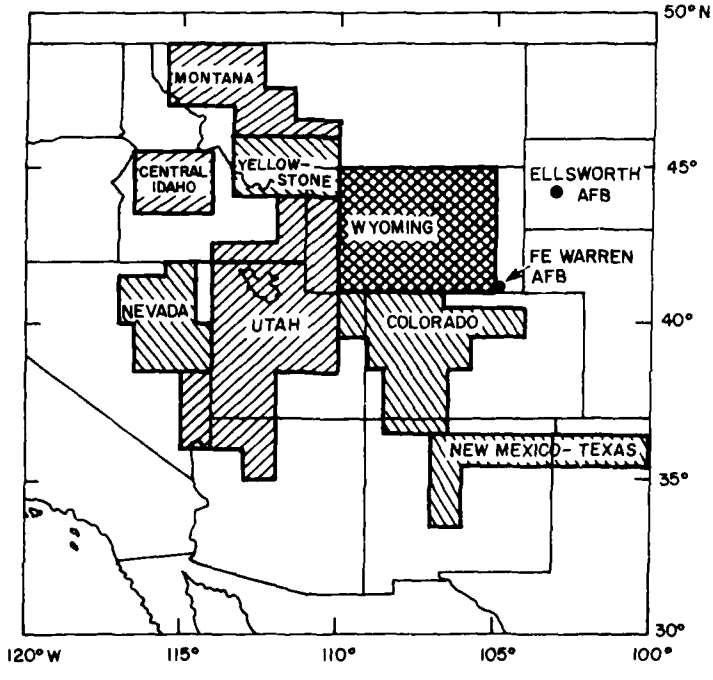

Figure 12. Seismic Source Regions Used to Evaluate the Seismic Hazard at Ellsworth and F. E. Warren Air Force Bases (indicated by closed circles)

The annual risk curves for Modified Mercalli intensity and peak ground acceleration, velocity, and displacement for Ellsworth AFB are displayed in Figures 13 and 14. Table 8 gives the ground motions calculated at specific levels of annual risk for Ellsworth AFB. A second set of peak acceleration, velocity, and displacement motion levels was constructed by conversion of the estimated site intensities. These values are given in Table 9. Given the limitations of calculating ground motions from site intensity, the two sets of values are considered in good agreement. This is especially true in that the site intensity values are only mean values at the specified intensities. For example, while the 0.001 annual risk accelerations appear to be significantly different the value calculated directly is within the 90 percent confidence bounds for site intensity V.

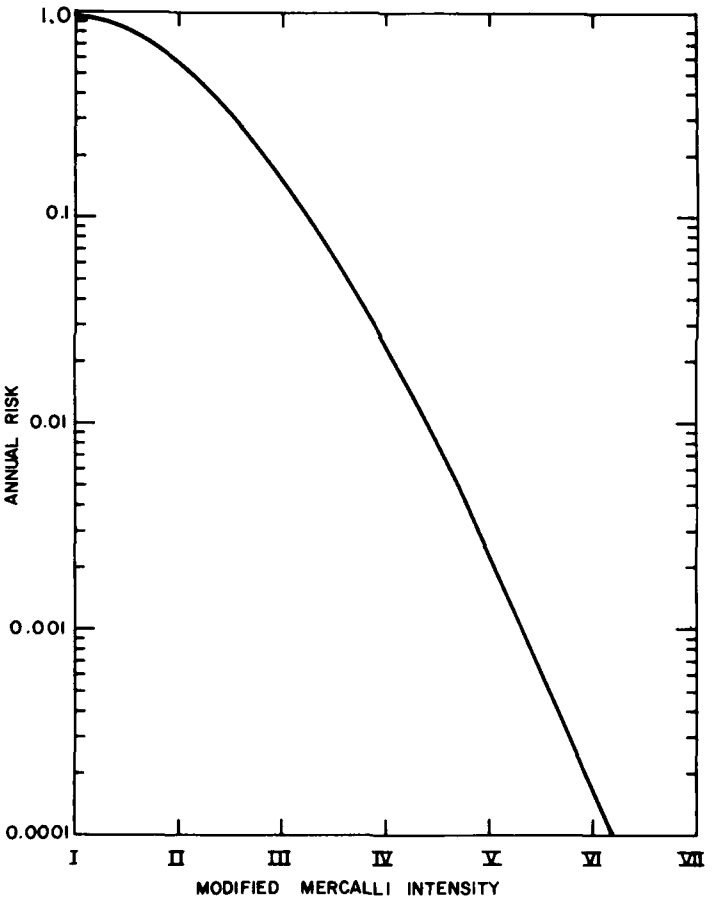

Figure 13. Modified Mercalli Intensity Seismic Risk Curve for Ellsworth AFB

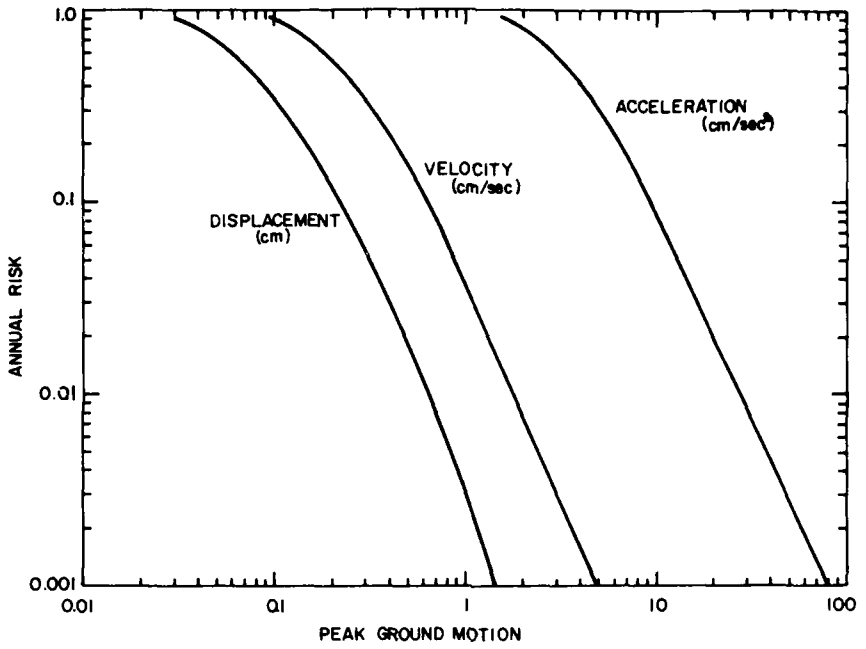

Figure 14. Peak Ground Acceleration, Velocity, and Displacement Seismic Risk Curves for Ellsworth AFB

Table 8. Peak Ground Motion Annual Risk Levels for Ellsworth AFB

Annual Risk	Return Period (years)	Intensity	Acceleration (cm/sec^2)	Velocity (cm/sec)	Displacement (cm)
0.9	1.11	I	1.6	0.1	0.03
0.5	2	II	3.4	0.2	0.07
0.2	5	II-III	6.4	0.4	0.14
0.1	10	III	9.3	0.6	0.21
0.05	20	III	13.1	0.9	0.29
0.02	50	IV	20.3	1.3	0.45
0.01	100	IV	27.9	1.8	0.60
0.005	200	IV	38.2	2.4	0.79
0.002	500	V	57.3	3.6	1.11
0.001	1000	V	77.2	4.8	1.42

Table 9. Peak Ground Motion Annual Risks Levels at Ellsworth AFB Based on Intensity Levels

Annual Risk	Fractional Intensity	Acceleration (cm/sec^2)	Velocity (cm/sec)	Displacement (cm)
0.9	1.1	2.1	0.4	0.1
0.5	2.1	4.0	0.8	0.2
0.2	2.8	6.5	1.1	0.3
0.1	3.2	8.8	1.5	0.4
0.05	3.6	11.4	1.8	0.5
0.02	4.1	15.8	2.4	0.7
0.01	4.4	19.3	2.8	0.8
0.005	4.7	23.5	3.3	1.0
0.002	5.0	30.6	4.2	1.2
0.001	5.3	37.5	4.9	1.4

For this wing, the acceleration levels for annual risk are, to a large degree, determined by the background seismicity characteristics. For peak velocity and displacement, which attenuate slower than acceleration, the seismic source regions in Wyoming and Colorado contribute to the risk in a greater amount. In neither case, however, do the nearest sources play a dominant role in establishing the seismic risk. In this case, the spatial change in seismic hazard is expected to be negligible. Little change in the acceleration values would be expected within 50 km of the site in any direction. Very gradual increases in velocity and displacement could be expected towards the southwest, as the defined sources are approached, but within 50 km the changes are not expected to be substantial.

In Figures 15a, 15b, and 15c, the 10-, 100-, and 1000-year return period composite horizontal design response spectra determined for Ellsworth AFB are shown. These spectra are based on the ground motion levels given in Table 8.

Twelve moderate sized earthquakes have been reported within 200 km of Ellsworth AFB between 1895 and 1978. The epicenters of these events are shown in Figure 16. The closest event was of magnitude 4.1 m_b and epicentral intensity VI located 34 km to the west of the base and occurred on 26 June 1968. The depicted events are erratically distributed in space and provide little information on future potential epicenters within this region. The maximum reported magnitude in this set of events was 5.1 m_b and epicentral intensity VII, both determined for the same event.

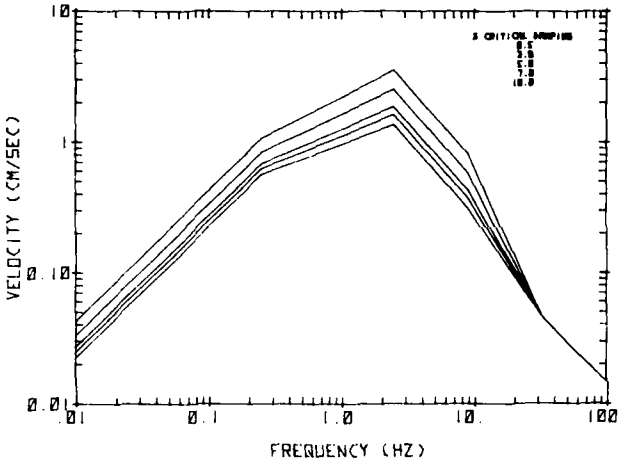

Figure 15a. Composite Horizontal Design Response Spectra for Ellsworth AFB Based on 10-year Return Period Ground Motions

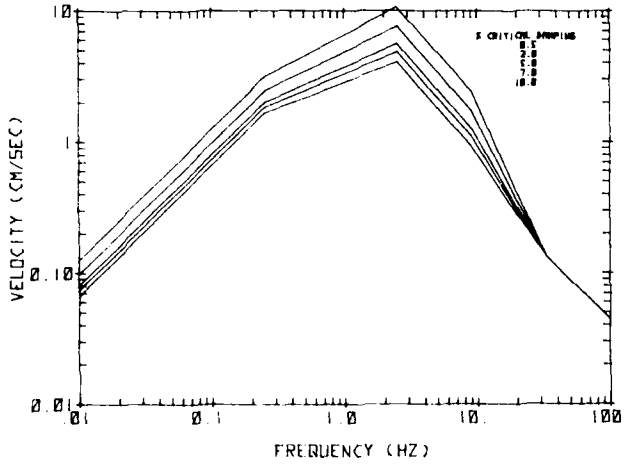

Figure 15b. Composite Horizontal Design Response Spectra for Ellsworth AFB Based on 100-year Return Period Ground Motions

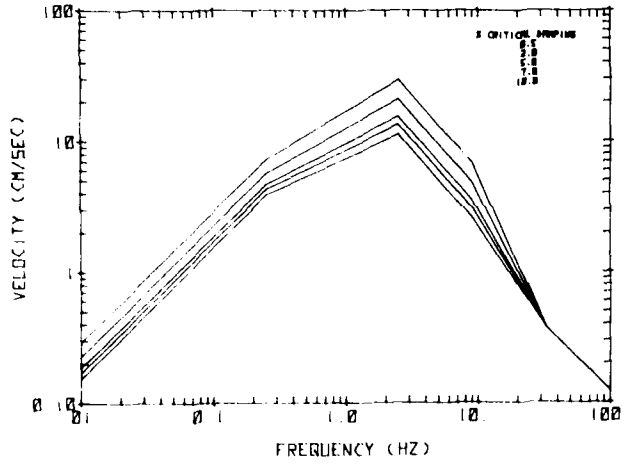

Figure 15c. Composite Horizontal Design Response Spectra for Ellsworth AFB Based on 1000-year Return Period Ground Motions

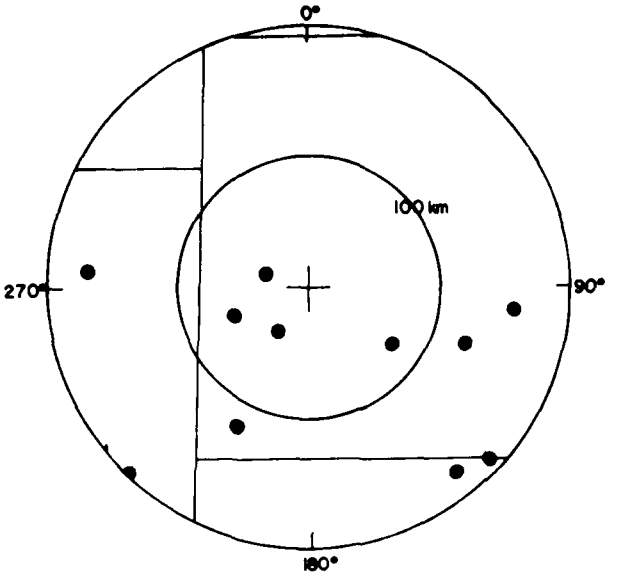

Figure 16. Reported Earthquake Epicenters
Within 200 km of Ellsworth AFB

3.3 Minot AFB and Grand Forks AFB – Wings III and VI

As with the previous studies a search of the NOAA Earthquake data file was made for all earthquakes within 1000 km of these two facilities. While 1100 events are located within that radius of Minot AFB, only 124 earthquakes were found in Grand Forks AFB. The difference in the number of reported events is due to the preponderance of earthquakes in the 600 to 1000 km range from Minot, including the activity from the Montana, Yellowstone, and portions of the Wyoming and Colorado source regions depicted in Figure 12. The seismic sources shown in this figure were used to evaluate the seismic risk at Minot AFB and portions of the last two were within the 1000 km radius used to evaluate the risk at Grand Forks AFB. The seismicity parameters for these source regions are given in Table 7.

Outside of these sources, the seismic activity within 1000 km of both bases has a low incidence of occurrence with a wide scatter of earthquake epicenters. Together these conditions make the identification of seismic trends or source areas impossible. In this situation it is necessary to assume that the activity occurs randomly throughout the entire region outside of explicit sources. All activity not included in the source regions listed above were lumped into one data set for evaluation of a single recurrence curve. This curve was used as the

background activity level for all sites except Whiteman AFB and the parameters of the curve are given in Table 7 under the label Background.

This assumption of random distribution of activity could be conservative in the sense that the activity is assumed to have an equal probability of occurring anywhere including at the site of interest. While the lack of sufficient knowledge concerning the earthquake activity in this region precludes any other approach, it is possible that the conditions required to generate an earthquake do not exist anywhere near the sites of interest and would produce a reduction of the seismic hazard at these wings.

It is apparent from the range of the closest seismic source region, approximately 500 km for Minot AFB and 750 km for Grand Forks AFB, that the background seismicity dominates the seismic hazard at each site and that the hazard is essentially equal at both facilities. The difference being so small that they must be considered negligible. In Figure 17, the site intensity risk curve for these bases is plotted and in Figure 18 the peak ground acceleration, velocity, and displacement curves are shown. The ground motion amplitudes at specific levels of annual risk are also given in Table 10 and in Table 11 the ground motion levels estimated on the basis of intensity are given. For acceleration the values are within a factor of two throughout the entire range and can be considered in good agreement. Both velocity and displacement tend to converge at the lower levels of risk but are substantially different at the higher risks.

In Figures 19a, 19b, and 19c, the composite horizontal response spectra for 10-, 100-, and 1000-year return period ground motions are shown. These figures are based on the ground motions given in Table 10.

The closest reported earthquake activity to either facility was an epicentral intensity IV earthquake reported at Williston, North Dakota on 26 October 1946 and was located approximately 175 km to the west of Minot AFB, nearly on the Montana-North Dakota state line. The nearest activity to Grand Forks AFB occurred on 23 December 1928 in north central Minnesota at an epicentral distance of 260 km. Each site is within 300 km of several other events all of which were small to moderate in magnitude with the largest event having an epicentral intensity of VII. As stated earlier, the locations of the activity is erratic and provides little information on the location of future activity near the facilities. The epicenters of the earthquakes within 300 km of Minot AFB and Grand Forks AFB are plotted in Figures 20 and 21, respectively. These events cover the period of 1917 to 1978.

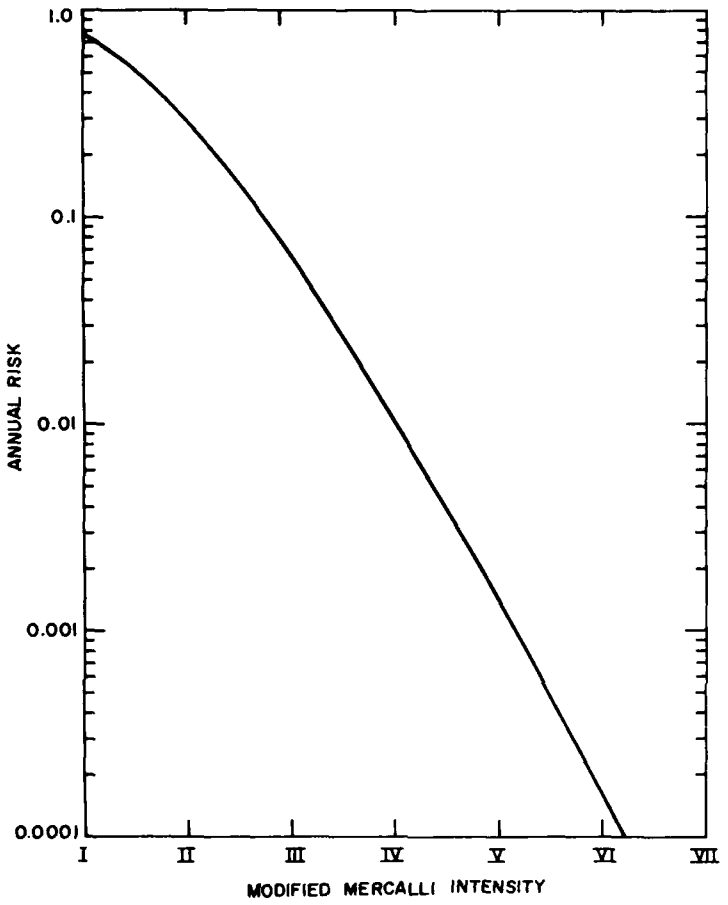

Figure 17. Modified Mercalli Intensity Seismic Risk Curves for Minot and Grand Forks Air Force Bases

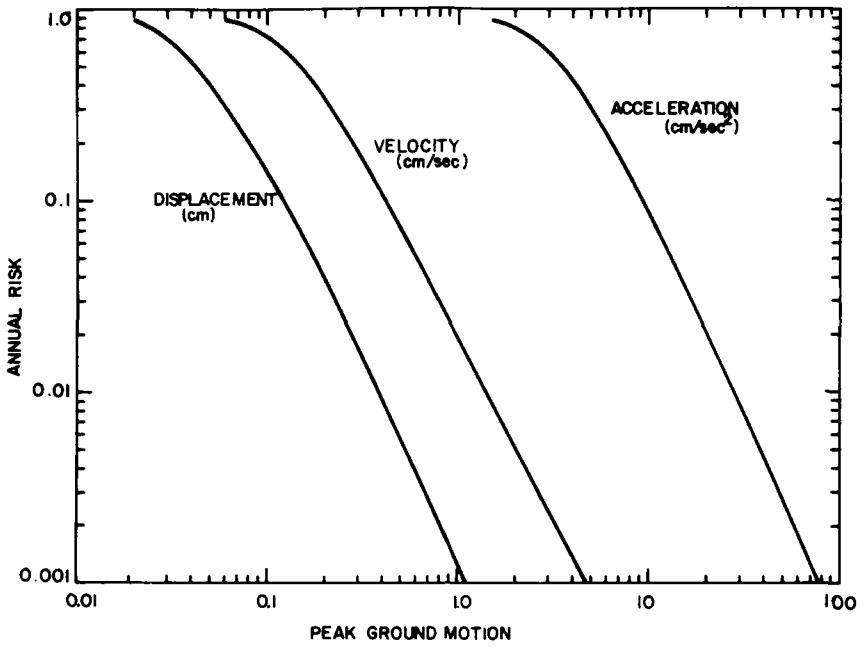

Figure 18. Peak Ground Acceleration, Velocity, and Displacement Seismic Risk Curves for Minot and Grand Forks Air Force Bases

Table 10. Peak Ground Motion Annual Risk Levels for Minot AFB and Grand Forks AFB

Annual Risk	Return Period (years)	Intensity	Acceleration (cm/sec^2)	Velocity (cm/sec)	Displacement (cm)
0.9	1.11	—	1.5	0.06	0.02
0.5	2	I	3.4	0.14	0.04
0.2	5	II	6.4	0.28	0.08
0.1	10	II	9.3	0.42	0.13
0.05	20	III	13.1	0.61	0.18
0.02	50	III	20.3	1.00	0.29
0.01	100	III-IV	27.9	1.43	0.40
0.005	200	IV	38.2	2.06	0.54
0.002	500	IV-V	57.3	3.30	0.82
0.001	1000	V	77.2	4.66	1.11

Table 11. Peak Ground Motion Annual Risk Levels at Minot AFB and Grand Forks AFB Based on Intensity Levels

Annual Risk	Fractional Intensity	Acceleration (cm/sec^2)	Velocity (cm/sec)	Displacement (cm)
0.9	---	---	---	---
0.5	1.4	2.63	0.54	0.17
0.2	2.2	4.55	0.85	0.26
0.1	2.7	6.18	1.10	0.33
0.05	3.1	8.27	1.40	0.41
0.02	3.6	11.56	1.85	0.54
0.01	4.0	13.93	2.16	0.63
0.005	4.3	19.14	2.82	0.81
0.002	4.8	26.85	3.74	1.06
0.001	5.2	34.20	4.57	1.28

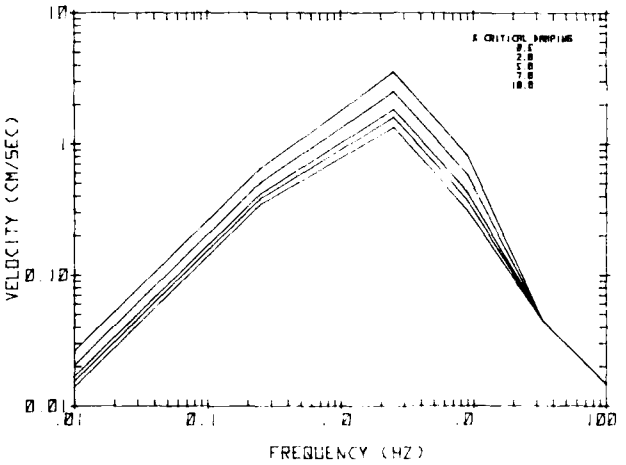

Figure 19a. Composite Horizontal Design Response Spectra for Minot and Grand Forks Air Force Bases Using 10-year Return Period Ground Motions

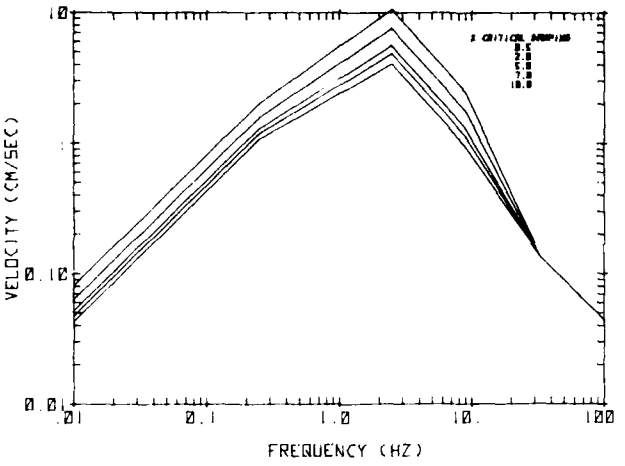

Figure 19b. Composite Horizontal Design Response Spectra for Minot and Grand Forks Air Force Bases Using 100-year Return Period Ground Motions

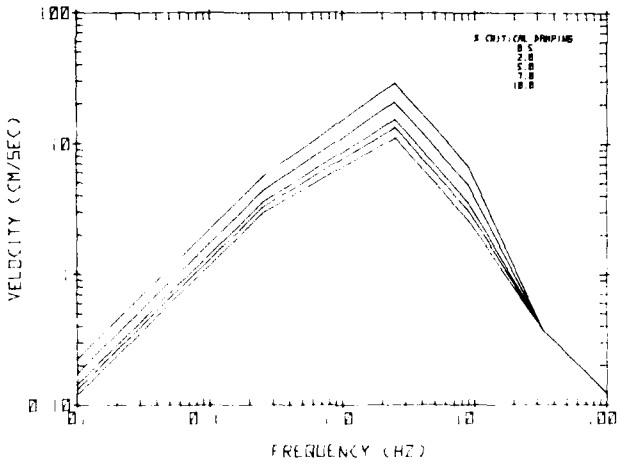

Figure 19c. Composite Horizontal Design Response Spectra for Minot and Grand Forks Air Force Bases Using 1000-year Return Period Ground Motions

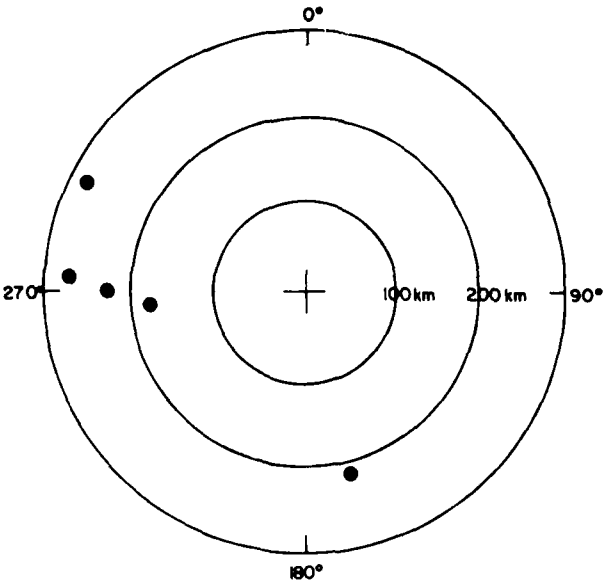

Figure 20. Reported Earthquake Epicenters Within 300 km of Minot AFB

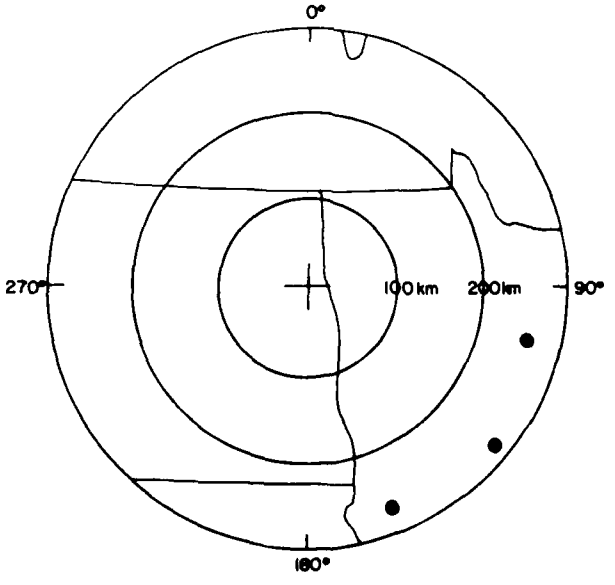

Figure 21. Reported Earthquake Epicenters Within 300 km of Grand Forks AFB

3.4 Whiteman AFB – Wing IV

Whiteman AFB is located near what is probably the most active seismic region in the United States east of the Rocky Mountains. The area near the confluences of the Ohio, Missouri, and Mississippi Rivers encompasses a large percentage of the epicenters of earthquakes reported in the central United States. Among the events reported in this region are several of the largest events to have occurred in the continental United States during historic times. The location of Whiteman AFB relative to this source region, the Central Mississippi Valley area, is shown in Figure 22. In addition to this source region, only a source region designated as the Southeastern United States has any extent within the 1000 km radius of Whiteman AFB. Outside of these two regions the seismic activity in the central United States appears to be randomly distributed and was treated as background seismicity. All risk calculations were conducted for 38.96°N and 92.35°W, the coordinates of Columbia, Missouri. As discussed at the end of Section 2.3, some modification of the risk estimate for this site is expected due to changes presently being made to the attenuation function modification procedure.

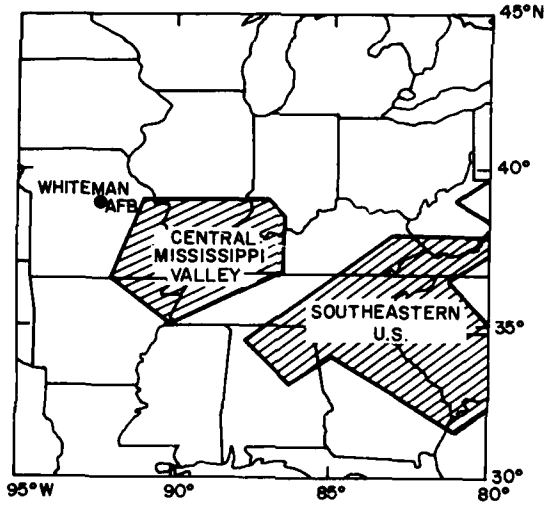

Figure 22. Seismic Source Regions Used in the Evaluation of Seismic Risk at Whiteman AFB (indicated by closed circle)

Previous seismicity studies have been conducted for both of the source regions included in risk evaluations for Whiteman AFB and these studies were used to define the recurrence curves for the source regions. The Southeastern United States source area was investigated by Bollinger.[13] The recurrence curve generated in this study was converted by Modified Mercalli intensity to local magnitude, M_L, using a relation derived for the eastern United States by Brazee.[14] For the Central Mississippi Valley region several studies have been conducted and the recurrence curves are in reasonable agreement.[15, 16, 17] The recurrence curves developed by Battis[17] for this source region and for the central United States background seismicity were used in this report. The parameters defining the seismic activity for these areas are given in Table 12.

Table 12. Whiteman AFB Source Region Parameters

Source	Area (10^4 km)	$\log (N/Y) = A - bM_L$		M_L MAX
		A	b	
Central Mississippi Valley	15.9	2.12	0.62	8.0
Southeastern United States	43.2	3.09	0.85	7.5
Background	----	-0.58†	0.56	6.0

†$\log (N/y/10^4\ km^2)$

The seismic hazard for Whiteman AFB was calculated using both site intensity and regionally modified acceleration attenuation functions for the central United States as given in Table 2. At present, no satisfactory independent means is available to estimate peak ground velocity or displacement risk curves for the central United States and these curves could only be obtained by scaling of either the acceleration or intensity risk curves. Scaling based on intensity is done using Eqs. (3), (4), and (5). Given the acceleration risk curve, velocity and displacement curves can be estimated using the "standard" earthquake values as determined by Newmark and Hall.[18] The "standard" earthquake assumes a ratio of acceleration to velocity and displacement of 0.5:60.96 cm/sec:45.72 cm. The same ratios are assumed for all other levels of acceleration. This procedure is open to question for several reasons. These ratios were determined by analysis of records of the 1940 Imperial Valley, California earthquake. The ratio of high frequency, motions, or acceleration, to longer period motions of velocity and displacement at the source

(Due to the large number of references cited above, they will not be listed here. See References, page 57.)

appear to be dependent on many factors such as fault rupture length, rise time, and stress drop which vary with the magnitude of the earthquake and regional tectonics. Away from the source, regional variation in frequency dependent attenuation will also affect the validity of these ratios. However, there does not appear to be a clearly superior method for evaluating the velocity and displacement risk curves.

The site intensity risk curves and evaluated peak acceleration and scaled velocity and displacement risk curves are shown, as the curves labeled "a", in Figures 23 and 24 respectively. Values of these ground motion descriptors at specified levels of annual risk are also given in Table 13. In Table 14, the equivalent peak ground motion values determined by conversion from site intensity are given. Comparison of the two sets of values given in Table 14 indicate a large discrepancy between the seismic hazard as indicated by site intensity and peak ground acceleration. To determine which risk curve is more reasonable, a comparison was made between the predicted recurrence periods for site intensities and the periods based on historic observations. The source for the historic data was a compilation by Brazee[14] covering a one-degree square, including Columbia, for the 45-year period from 1928 to 1973.

Historically, the Columbia area has experienced intensity III or greater six times, IV or greater on four occasions, two V or greater, and one intensity VI during this period. The intensity based risk curve predicts 24 occurrences of III or greater, 12 of IV or larger, 6 V or greater, 2 intensity VI or greater and 1 intensity VII or larger earthquake. Though the actual historic and predicted rates should not be expected to parallel exactly, the departure between historic record and prediction is significant especially at the low intensities which, due to the frequency of occurrence should be reflected more accurately in the risk curve. Using Eq. (3) the mean value of acceleration at each intensity can be determined and the expected number of occurrences in the 45-year period determined. These calculations yield 9, 4, 2 and 1 occurrences of intensities III, IV, V and VI or greater, respectively, at Whiteman AFB. While this comparison is only approximate, it suggests that the intensity risk curve overstates the risk at Whiteman AFB and the acceleration risk curve appears to be more realistic in representing the ground motions experienced at this facility.

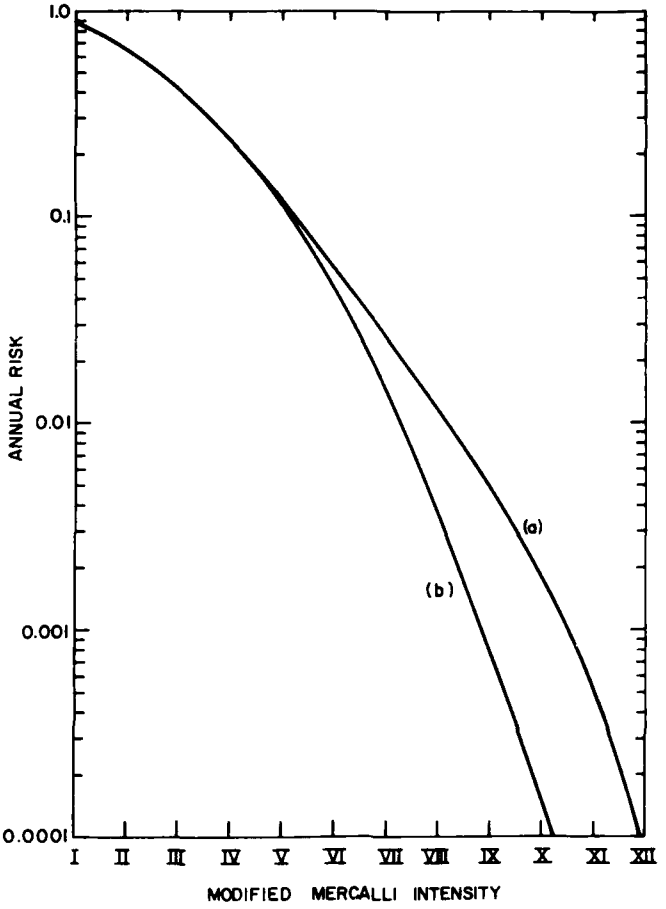

Figure 23. Modified Mercalli Intensity Seismic Risk Curves for Whiteman AFB. Curve (a) assumes the maximum magnitude earthquake can occur anywhere in the Central Mississippi Valley source region. Curve (b) restricts this event to the southern extent of the source region. See text for fuller discussion.

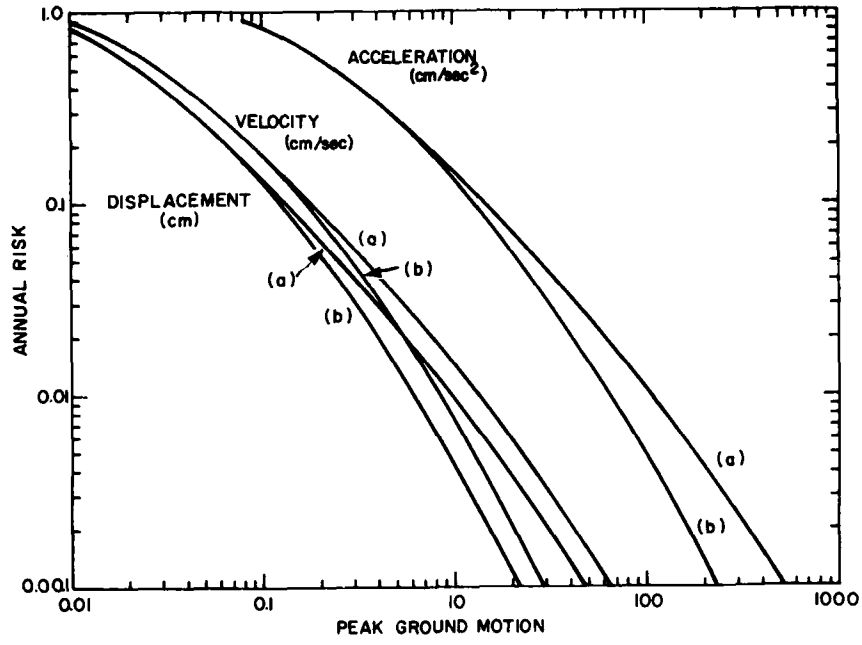

Figure 24. Peak Ground Acceleration, Velocity, and Displacement Seismic Risk Curves for Whiteman AFB. Curves labeled (a) assume the maximum magnitude earthquake can occur anywhere in the Central Mississippi Valley source region. Curves labeled (b) restrict this event to the southern extent of the source region. See text for fuller discussion

Table 13. Peak Ground Motion Annual Risk Levels for Whiteman AFB

Annual Risk	Return Period (years)	Intensity	Acceleration (cm/sec^2)	Velocity (cm/sec)	Displacement (cm)
0.9	1.11	---	0.8	0.1	0.1
0.5	2	II	2.5	0.3	0.2
0.2	5	IV	7.2	0.9	0.7
0.1	10	V	14.0	1.7	1.3
0.05	20	VI	26.4	3.3	2.5
0.02	50	VII	58.7	7.3	5.5
0.01	100	VIII	104.5	13.0	9.8
0.005	200	IX	178.8	22.3	16.7
0.002	500	X	335.3	41.8	31.4
0.001	1000	X	509.0	63.4	43.6

Table 14. Peak Ground Motion Annual Risk Levels for Whiteman AFB Based on Intensities

Annual Risk	Fractional Intensity	Acceleration (cm/sec^2)	Velocity (cm/sec)	Displacement (cm)
0.9	-----	-----	-----	-----
0.5	2.6	5.8	1.0	0.3
0.2	4.2	17.7	2.6	0.8
0.1	5.2	35.2	4.7	1.3
0.05	6.1	65.0	7.8	2.1
0.02	7.3	152.1	15.8	4.2
0.01	8.2	279.3	26.3	6.9
0.005	9.0	498.9	42.7	11.0
0.002	10.0	968.0	74.1	18.6
0.001	10.53	1396.4	100.6	25.0

As with most of the areas studied in this report the direct correlation of earthquake epicenters with known faults in the Central Mississippi Valley region is not possible at the present time. In this sense, the boundaries of source region are arbitrary in their assignment. To indicate the possible variation in the seismic hazard at Whiteman AFB due to this factor a contour plot of the 500-year return period accelerations for a one-degree square centered on Whiteman AFB is shown in Figure 25. By reciprosity, expansion of the source region towards the base is equivalent to moving the base towards the source. Conversely, reduction of the source area is equivalent to moving the site of interest to the northwest of its present location. The gradient in this region is not very steep and changes of the order of a few tens of kilometers in the bounds of the Central Mississippi Valley source region would not substantially change the seismic hazard estimate at Whiteman AFB.

A second potential modifier of the risk curves involves the non-uniformity of earthquake activity within the Central Mississppi Valley source region. Insufficient data is presently available to subdivide this region into smaller areas, and thus account for the non-uniformity of the activity. However, another approach was used to obtain a limiting lower bound to the risk curves. It was assumed that the earthquake process in much of the Central Mississippi Valley source region could not generate the maximum magnitude earthquake of 8.0 M_L for this region. These large events were restricted to a region at the southern end of the source area in the vicinity of the Missouri - Arkansas - Tennessee junction. For the remainder of the source area a maximum magnitude earthquake of 6.5 M_L was allowed. The seismic risk curves for this case are given in Figures 23 and 24 as the curves

labeled "b". In Table 15, the ground motion levels at specified annual risks are given. These should be considered only as the lower limiting risk with the true curve lying somewhere between these two curves.

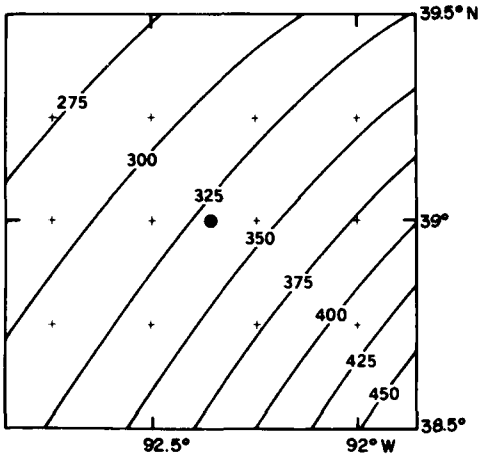

Figure 25. Contours of the 500-year Return Period Accelerations in a One-degree Square centered on Whiteman AFB (closed circle); (units of cm/sec^2). Accelerations calculated assuming the maximum magnitude earthquake can occur anywhere within the Central Mississippi Valley source region

Table 15. Lower Limit Peak Ground Motion Annual Risk Levels of Whiteman AFB

Annual	Return Period	Intensity	Acceleration (cm/sec^2)	Velocity (cm/sec)	Displacement (cm)
0.9	1.11	-----	0.8	0.1	0.1
0.5	2	II	2.5	0.3	0.2
0.2	5	IV	6.9	0.9	0.7
0.1	10	V	13.0	1.6	1.2
0.05	20	V-VI	22.7	2.8	2.1
0.02	50	VI-VII	43.8	5.5	4.1
0.01	100	VII	67.7	8.4	6.3
0.005	200	VII-VIII	100.7	12.6	9.4
0.002	500	VIII	161.5	20.1	15.1
0.001	1000	VIII-IX	224.7	28.0	21.0

The composite horizontal design response spectra for 10-, 100-, and 1000-year return periods are shown in Figures 26a, 26b, and 26c. These spectra are based on the ground motions given in Table 13 which assumed a uniform potential for a magnitude 8.0 M_L earthquake throughout Central Mississippi Valley Source Region.

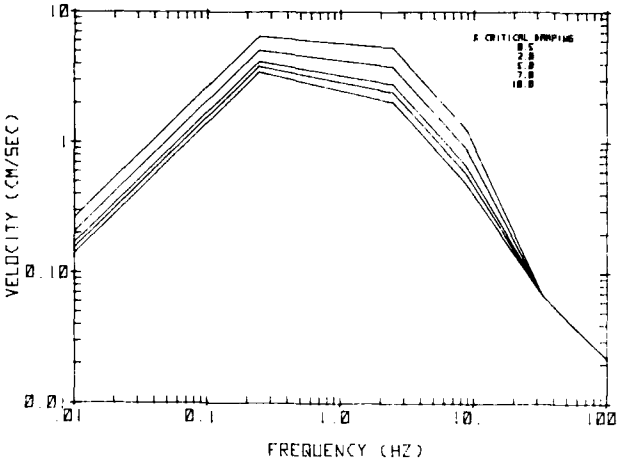

Figure 26a. Horizontal Design Response Spectra for Whiteman AFB Based on 10-year Return Period Ground Motions Assuming the Maximum Magnitude Earthquake Can Occur Anywhere in the Central Mississippi Valley Source Region

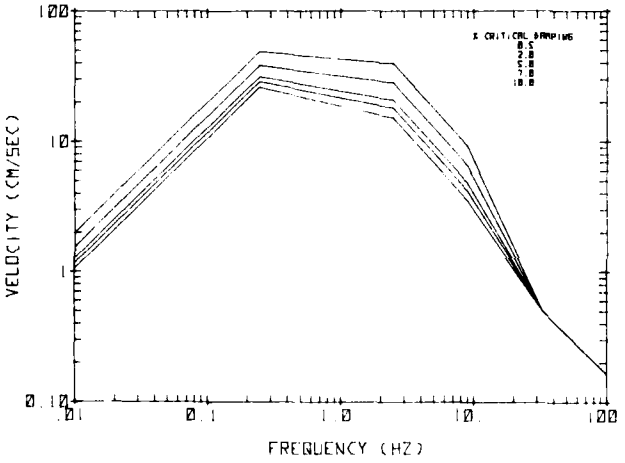

Figure 26b. Horizontal Design Response Spectra for Whiteman AFB Based on 100-year Return Period Ground Motions Assuming the Maximum Magnitude Earthquake Can Occur Anywhere in the Central Mississippi Valley Source Region

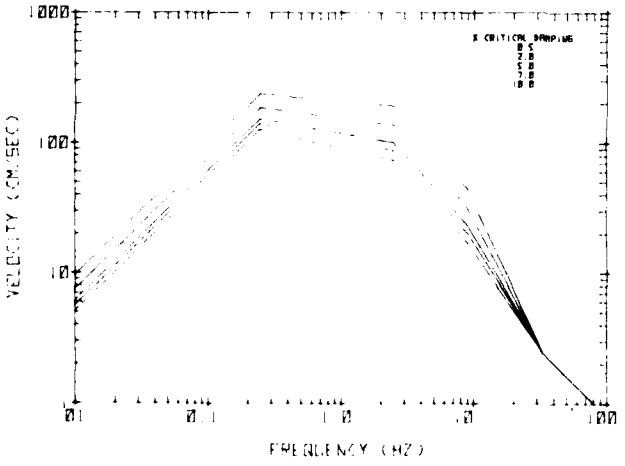

Figure 26c. Horizontal Design Response Spectra for Whiteman AFB Based on 1000-year Return Period Ground Motions Assuming the Maximum Magnitude Earthquake Can Occur Anywhere in the Central Mississippi Valley Source Region

In Figure 27, all earthquakes reported in the Earthquake Data File with epicenters within 200 km of Whiteman AFB are plotted. Of these 27 events, the largest reported magnitude is one of 5.6 m_b which occurred in March 1974 at a distance of 198 km from the base. The nearest event is at 108 km but has no reported magnitude or intensity. The concentration of epicenters to the southeast of Whiteman AFB lays within the Central Mississippi Valley seismic source zone. Several earthquakes not shown in this figure should also be noted. The most important of these was the 1811-1812 series of shocks which occurred near New Madrid, Missouri in southeastern Missouri and northeastern Arkansas. Nuttli estimated the magnitude of the three principal shocks to be 7.3, 7.1 and 7.4 m_b.[19] In the meizoseismal zone it is thought that Modified Mercalli intensity XII was reached. The first of these events was reported felt as far away as Boston at an epicentral distance of approximately 1800 km.[20]. For purposes of comparison, the area enclosed in the Modified Mercalli intensity V isoseismal was estimated by Nuttli to be 2.5×10^6 km^2 while the 1960 San Francisco earthquake produced this intensity over an area of only 1.5×10^5 km^2.[19] Assuming that the maximum magnitude earthquake, 8.0 M_L, were to reoccur near the epicenter of these events, the predicted ground motions at Whiteman AFB would be approximately 428 cm/sec^2, 53 cm/sec and 40 cm. This corresponds to a site intensity of VIII - IX, approximately one unit higher than that obtained by extrapolation of Nuttli's isoseismal map for the first event in this series.[19] The horizontal design response spectra for this event does not exceed the 1000-year return period spectra shown in Figure 26c.

3.5 F.E. Warren AFB – Wing V

The seismic source regions used in the hazards evaluation for F.E. Warren AFB are identical to those used for Ellsworth AFB and are shown in Figure 12. These regions are based on an examination of all seismic activity within 1000 km of the facility. The associated seismicity parameters for these areas are given in Table 7. The coordinates of Cheyenne, Wyoming, 41.1°N and 104.9°W were used as the location for which the seismic risk was calculated.

The annual risk curves for F.E. Warren AFB, for Modified Mercalli intensity and peak ground acceleration, velocity, and displacement are shown in Figures 28 and 29, respectively. As with all sites except for Whiteman AFB, each risk curve is independently evaluated using the appropriate attenuation function as specified

19. Nuttli, O. (1973) The Mississippi Valley earthquakes of 1811 and 1812: Intensities, ground motion and magnitudes, Bull. Seism. Soc. Am. 63:227-248.

20. Von Hake, C. (1974) Earthquake history of Missouri, Earthquake Information Bull. 6:25-26.

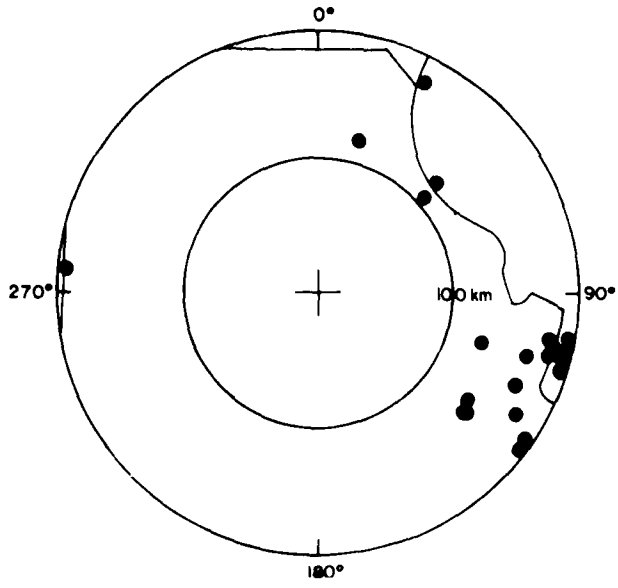

Figure 27. Reported Earthquake Epicenters Within 200 km of Whiteman AFB

in Table 2. For specific levels of annual risk, the calculated ground motions at F. E. Warren AFB are given in Table 16. In Table 17 the ground motions for these same annual risks, as evaluated by conversion of site intensities, are given. The two sets of values, given the limitations of the conversion procedure, are considered to be in reasonable agreement. The ground motions calculated directly, however, are the preferred values.

As can be seen in Figure 12 the location of F. E. Warren AFB is in close proximetry to the boundaries of two source regions, those designated as Colorado and Wyoming in this figure. In Figure 30 the contours of the 500-year year return period accelerations within a one-degree square centered on Wing V are shown. The general characteristics of this field also hold for other risk levels and ground motion parameters though typically the gradient is shallower. Beyond the spatial variation of seismic risk in the vicinity of F. E. Warren AFB, this figure also provides information on the effects of relocation of the borders of the Colorado and Wyoming source regions. Movement of the site towards or away from the boundary of these source regions is equivalent to moving the borders relative to the site. As these borders are arbitrarily assigned due to various factors discussed in Section 2 of this report, this figure provides an indication of the uncertainty in the risk evaluation which is associated with these factors.

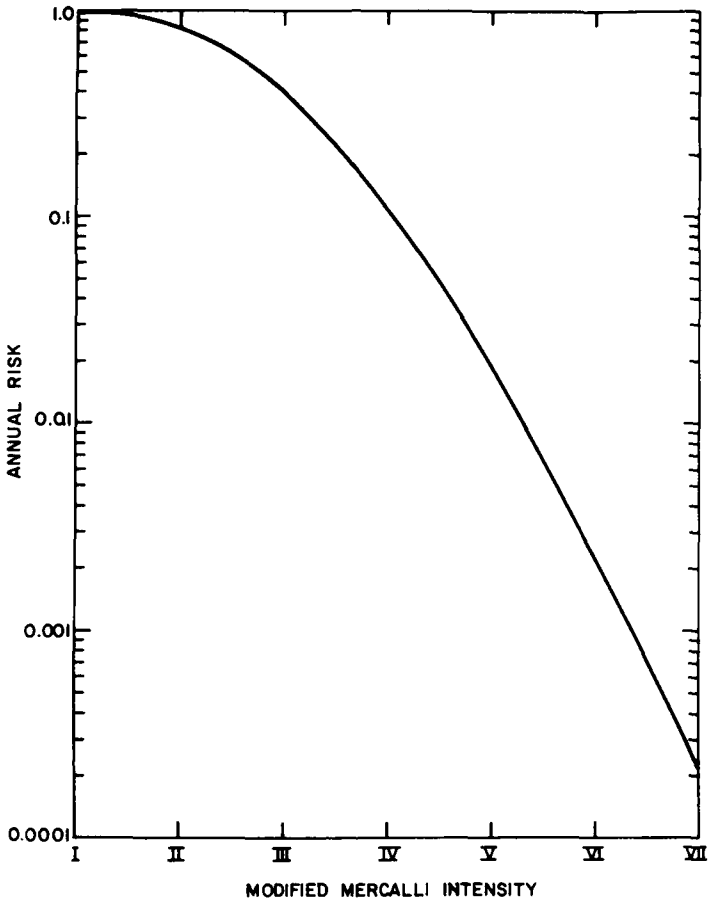

Figure 28. Modified Mercalli Intensity Seismic Risk Curve for F. E. Warren AFB

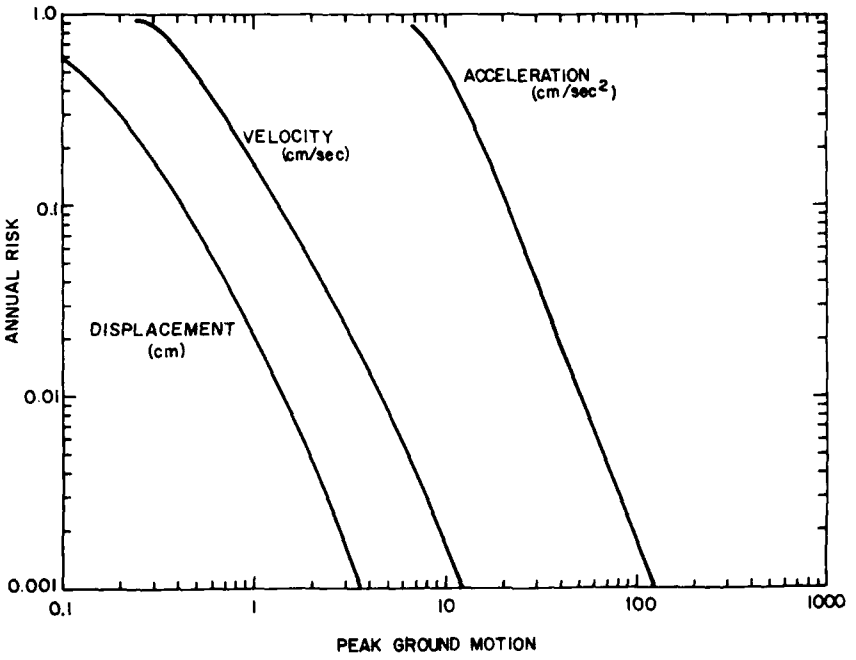

Figure 29. Peak Ground Acceleration, Velocity, and Displacement Seismic Risk Curves for F. E. Warren AFB

Table 16. Peak Ground Motion Annual Risk Levels for F. E. Warren AFB

Annual Risk	Return Period (years)	Intensity	Acceleration (cm/sec^2)	Velocity (cm/sec)	Displacement (cm)
0.9	1.11	I-II	6.7	0.2	0.05
0.5	2	II	10.8	0.5	0.13
0.2	5	III	16.1	0.9	0.26
0.1	10	IV	21.0	1.4	0.41
0.05	20	IV	27.3	2.0	0.61
0.02	50	IV-V	38.5	3.3	0.97
0.01	100	V	50.1	4.5	1.35
0.005	200	V	65.3	6.3	1.84
0.002	500	VI	93.1	9.3	2.70
0.001	1000	VI	121.8	12.4	3.55

Table 17. Peak Ground Motion Annual Risk Levels for F. E. Warren AFB Based on Intensity Levels

Annual Risk	Fractional Intensity	Acceleration (cm/sec^2)	Velocity (cm/sec)	Displacement (cm)
0.9	1.8	3.3	0.7	0.2
0.5	2.7	6.3	1.1	0.3
0.2	3.5	11.1	1.8	0.5
0.1	4.0	15.7	2.4	0.7
0.05	4.4	20.7	3.0	0.9
0.02	5.0	29.9	4.1	1.2
0.01	5.3	37.7	5.0	1.4
0.005	5.6	47.4	6.0	1.7
0.002	6.1	63.8	7.7	2.1
0.001	6.4	78.0	9.1	2.5

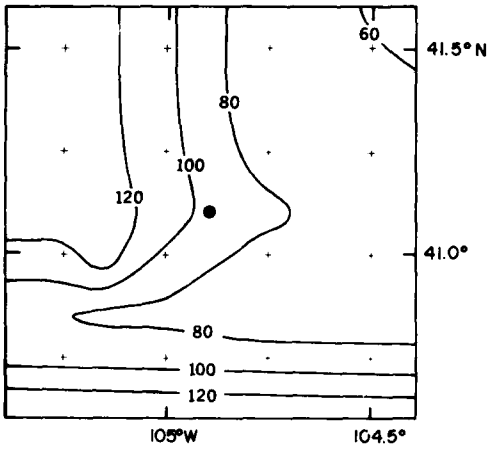

Figure 30. Contours of the 500-year Return Period Acceleration in a One-degree Square Centered on F. E. Warren AFB (closed circle). (Units of cm/sec^2)

In Figures 31a, 31b, and 31c the composite horizontal design response spectra for 10-, 100-, and 1000-year return period ground motions as given in Table 15, are shown.

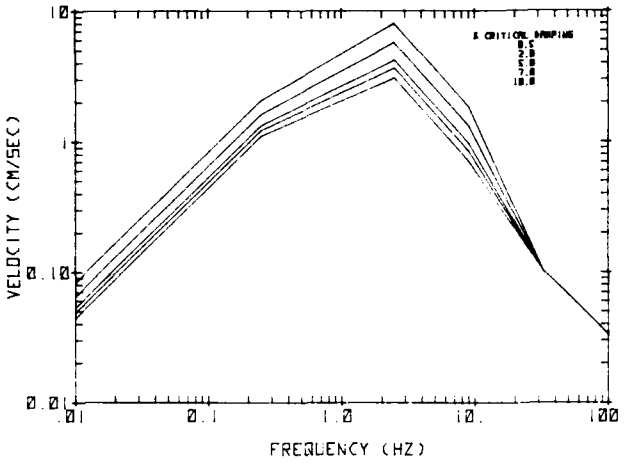

Figure 31a. Composite Horizontal Design Response Spectra for F. E. Warren AFB Based on 10-year Return Period Ground Motions

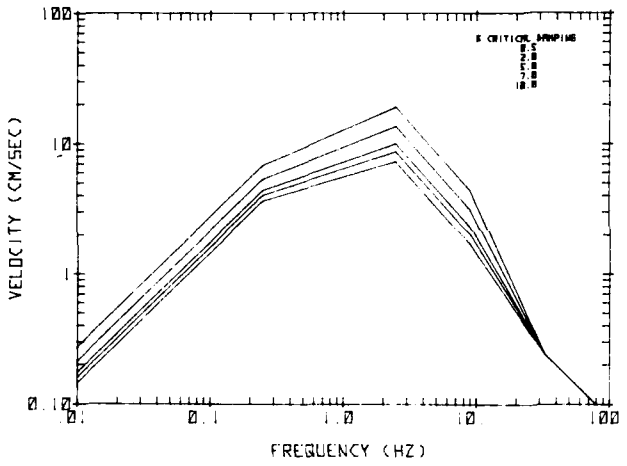

Figure 31b. Composite Horizontal Design Response Spectra for F. E. Warren AFB Based on 100-year Return Period Ground Motions

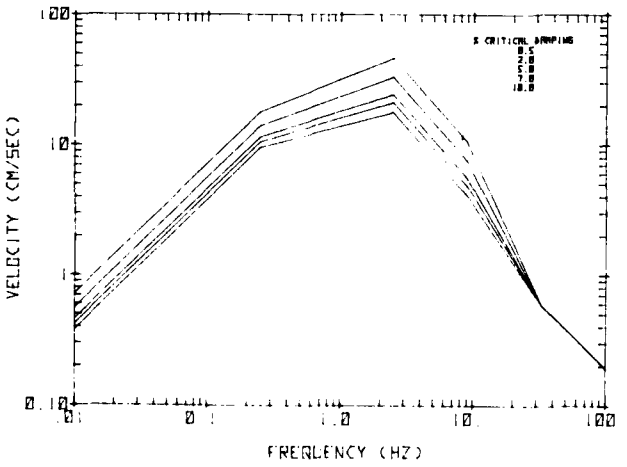

Figure 31c. Composite Horizontal Design Response Spectra for F. E. Warren AFB Based on 1000-year Return Period Ground Motions

Figure 32 is a plot of all earthquakes which have occurred within 200 km of F. E. Warren AFB. A total of 63 events are plotted covering a period from 1892 to 1978. The closest event was located approximately 8 km from the site of interest but had no reported magnitude or intensity. The largest event is one of magnitude 5.3 m_b and epicentral intensity of VII which occurred in August 1967. It was located at 135 km from F. E. Warren AFB in the cluster of epicenters due south of the site. The vast majority of the events reported have body-wave magnitudes between 4.0 and 5.3 m_b and were reported since 1963. Only five earthquakes are reported prior to 1963 indicating the incompleteness of the data set.

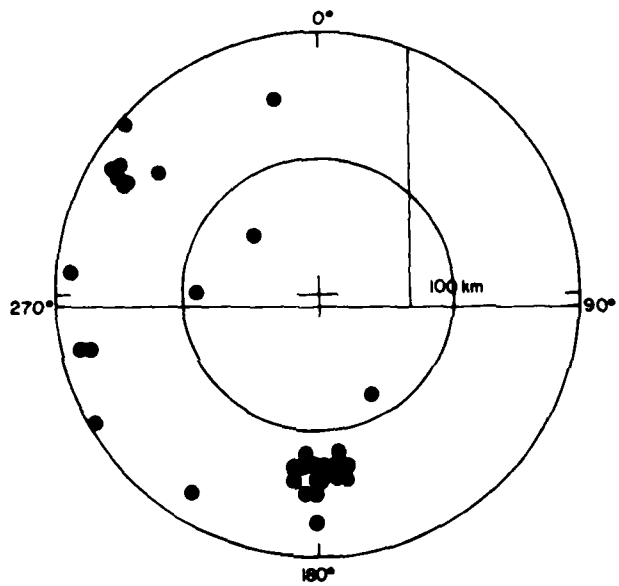

Figure 32. Reported Earthquake Epicenters Within 200 km of F. E. Warren AFB

Virtually all of the activity located in the cluster due south of the site is associated with fluid injection at the Rocky Mountain Arsenal outside of Denver, Colorado. It is assumed that the deep well injection of waste fluids from the Arsenal operation acted as a lubricant on faults within this region and allowed the rupturing of faults which would otherwise have remained locked until greater stresses could have accumulated. In a sense, this indicates that the inclusion of area in the Colorado source region may be inappropriate as these appear to be

induced earthquakes. However, at least two earthquakes have occurred in this region prior to the fluid injections, in 1882 and 1924, and the post-injection activity itself suggests that accumulation of sufficient strain in this region for significant future seismic activity. Thus, it is felt that this area should be included in the Colorado source region.

4. CONCLUSIONS

Using standard methods of probabilistic seismic risk analysis, estimates of the seismic hazard at six Minuteman missile wings were conducted. For four of the six sites, the dominant contribution to the site hazard is the general background seismicity. These sites were Malstrom, Ellsworth, Minot, and Grand Forks Air Force Bases. The background activity is used to represent earthquakes which appear to occur randomly throughout the regions surrounding the sites and which can not be associated with any distinct source region. The apparent randomness of these events is, at least in part, the result of low rates of occurrence and a short historical record which, taken together, greatly limit the ability of the investigator to isolate these events within a source region. The assumption of random occurrence for these events which was used in these studies, is to some degree, conservative as this activity may be more limited in areal extent and thus the estimated risk curves may also be conservative.

The site having the greatest seismic hazard is Whiteman AFB, Missouri. Though not commonly considered to be a region of high seismic hazard due to the lack of recent major earthquakes, the combination of low seismic wave attenuation in the central United States and the potential for major earthquakes in the central Mississippi Valley combine to produce high expected ground motions at this site for long inter-occurrence periods. For short return periods, less than 20 years, the expected ground motions are lower than those at the western United States missile wings. The uncertainties in ground motion estimates for this region are larger than for the west coast and it is expected that future studies will modify the results presented in this report. The changes presently being incorporated into the technique used to generate the peak acceleration attenuation function which was used for this site are expected to reduce the seismic hazard although a quantitative evaluation of the effect is not possible at present.

F. E. Warren AFB has the highest level of risk at the remaining sites. Both for this wing and for Malstrom AFB, significant changes in the predicted levels of risk can be obtained by relatively minor changes in the boundaries of close seismic source regions. As the boundaries of these regions are not well established, the variability associated with alteration of the boundaries must be considered in any application of these risk estimates.

References

1. Richter, C. (1958) Elementary Seismology, W.H. Freeman and Co., San Francisco, CA.

2. Stepp, J. (1972) Analysis of completeness of the earthquake sample in the Puget Sound area and its effect on statistical estimates of earthquake hazards, Proceedings of the International Conference on Microzonation for Safer Construction Research and Application, Seattle, WA.

3. McGuire, R. (1979) Adequacy of simple probability models for calculating felt shaking hazard using the Chinese earthquake catalog, Bull. Seism. Soc. Am. 69:877-892.

4. Quittmeyer, R., and Jacob, K. (1979) Historical and modern seismicity of south-central Asia, Bull. Seism. Soc. Am. 69:773-823.

5. Meyers, H., and von Hake, C. (1976) Earthquake Data File Summary, National Geophysical and Solar-Terrestrial Data Center Report KGRD-5.

6. Trifunac, M., and Brady, A. (1975) on the correlation of seismic intensity scales with peaks of recorded strong ground motion, Bull. Seism. Soc. Am. 65:139-162.

7. McGuire, R. (1976) FORTRAN Computer Program for Seismic Risk Analysis U.S. Geol. Surv. Open-File Report 76-67.

8. Orphal, D., and Laboud, J. (1974) Prediction of peak ground motion from earthquakes, Bull. Seism. Soc. Am. 64:1563-1574.

9. Cornell, C. (1968) Engineering seismic risk analysis, Bull. Seism. Soc. Am. 58:1503-1606.

10. Hays, W., Algermissen, S., Estinesa, A., Perkins, D., and Rinehart, W. (1975) Guidelines for Developing Design Earthquake Response Spectra, U.S. Geol. Surv. Technical Report M-114.

11. Battis, J. (1978a) Geophysical Studies for Missile Basing Seismic Risk Studies in the Western United States, Texas Instruments Inc., Scientific Report No. 2, ALEX(02)-ISR-78-01.

12. Neumann, F. (1937) United States Earthquakes, 1935. Department of Commerce, Coast and Geodetic Survey, Serial No. 600.

13. Bollinger, G. (1973) Seismicity of the southeastern United States, Bull. Seism. Soc. Am. 63:1785-1808.

14. Brazee, R. (1976) An Analysis of Earthquake Intensities With Respect to Attenuation, Magnitude, and Rate of Recurrence, National Geophysical and Solar-Terrestrial Center, NOAA Technical Memorandum EDS NGSDC-2.

15. Algermissen, S. (1972) The seismic risk map of the United States: Development use, and plans for future refinement. Conference on Seismic Risk Assessment for Building Standards, Washington, D.C.

16. Nuttli, O. (1974) Magnitude-recurrence relation for central Mississippi Valley earthquakes, Bull. Seism. Soc. Am. 64:1189-1207.

17. Battis, J., and Hill, K. (1977) Analysis of Seismicity and Tectonics of the Central and Western United States, Texas Instruments Inc., Interim Scientific Report ALEX(02)-ISR-77-01.

18. Newmark, N., and Hall, W. (1969) Seismic design criteria for nuclear reactor facilities, Fourth World Conference on Earthquake Engineering, Santiago, Chile.

19. Nuttli, O. (1973) The Mississippi Valley earthquakes of 1811 and 1812: Intensities, ground motion and magnitudes, Bull. Seism. Soc. Am. 63:227-248.

20. Von Hake, C. (1974) Earthquake history of Missouri, Earthquake Information Bull. 6:25-26.

Appendix A

Regional Modification of Acceleration Attenuation Functions

A1. INTRODUCTION

To convert the spatial and temporal characteristics of seismic activity into an estimate of the seismic hazard at the site of interest it is necessary to have a method for the determination of ground motion at a location remote from the epicenter of an earthquake of specified magnitude. A general set of functions of the form:

$$g_s = G(M, R) \tag{A1}$$

where g_s is the ground motion at the site of interest, M is the earthquake magnitude and R is the site epicentral or hypocentral distance, have been derived empirically for this purpose. Typically, the ground motion descriptor, g_s, is in terms of peak acceleration, velocity, or displacement; though other measures have been used (McGuire, 1976).

A problem of great significance is associated with the use of these functions. Most of the data upon which these equations are based are obtained in California. Only a very limited number of strong motion records are available from the rest of the continental United States. At the same time, there are many lines of evidence that ground motion attenuation in California is atypical compared to other

Note: See page 72 for Appendix A References.

areas of the United States (Brazee, 1976; Nuttli, 1973). Thus, the direct application of attenuation functions based primarily on western United States observations to other regions is at best only a gross approximation of the real situation.

A2. PAST MODIFICATION SCHEMES

Several methods have been suggested to overcome the difficulties of regional variation in ground motion attenuation. The first solution was the use of Modified Mercalli intensity as the ground motion descriptor, g_s. Intensity attenuation functions of the form:

$$I_s = I(M, r) \text{ or } I(I_o, R) \tag{A2}$$

where I_s is the site intensity and I_o the epicentral intensity, replaced the ground motion attenuation functions. The advantage of this method is that historical reports of earthquake damage can be interpreted in terms of Modified Mercalli intensity, greatly expanding the data base for analysis as compared to the use of ground motion descriptors requiring instrumental observations. This feature is significant for areas of low seismicity such as the central or eastern United States. In addition, the use of intensity appears to eliminate the dependence on western United States data to estimate seismic hazard.

This method, however, is highly unsatisfactory. The primary problem with this technique is that Modified Mercalli intensity describes ground motion on a very coarse scale which is based on subjective evaluations of damage. Taken alone, intensity is extremely difficult to interpret in terms of the engineering implications. What knowledge that does exist of the engineering parameters associated with given levels of Modified Mercalli intensity is, to a large degree, based on studies of western United States earthquakes. Thus, the method does not eliminate the cross-regional comparisons.

To eliminate the engineering application problems of using intensity, attempts have been made to correlate site intensity directly with peak acceleration, velocity, and displacement (Guttenberg and Richter, 1943; Trifunac and Brady, 1975; McGuire, 1977). Given a correlation between one of the ground motion parameters and site intensity:

$$g_s = f(I_s) \tag{A3}$$

it would be possible to convert the intensity attenuation functions to ground motion attenuation as:

$$g_s = f(I(M, R)) . \quad (A4)$$

It is obvious from the data shown in Figure A1 that the expected trends, increasing ground motion amplitude with increasing site intensity, occur on the average. However, the wide spread of values observed for a given intensity level result in only weak correlations between each of the ground motion parameters and intensity (Trifunac and Brady, 1975; McGuire, 1977; and Murphy and O'Brien, 1977). Velocity does correlate with intensity to a higher degree than acceleration or displacement. Unfortunately, most seismic engineering codes are written in terms of acceleration

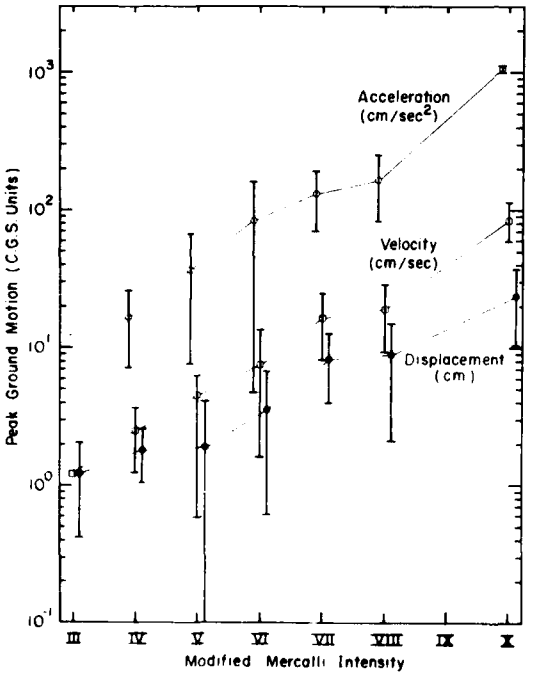

Figure A1. Means of Observed Peak Ground Acceleration, Velocity, and Displacements, With One Standard Deviation Error Bars, Plotted Against Modified Mercalli Intensity

In part, the low correlation can be explained by the coarseness of the Modified Mercalli intensity scale. Another significant element, however, is the dispersion of the wave train as it travels away from the epicenter. The level of damage which results from a single, impulsive motion can also result from a lower amplitude motion acting over more cycles. To incorporate this distance effect, correlations have also been made using both site intensity and epicentral distance:

$$g_s = G(I_s, R) . \tag{A5}$$

The use of distance significantly improves the correlation with peak acceleration and, to a lesser degree, with peak displacement (McGuire, 1977; Murphy and O'Brien, 1977).

Still, the use of either type of site intensity-ground motion relationship, Eqs. (A3) or (A5), outside of California, in conjunction with a regional intensity attenuation function, provides only limited improvement over the direct application of California based ground motion attenuation functions. In both cases, the effect of distance has not been completely removed. In the first form, the distance effects are completely ignored. In the second type of relationship, an assumption is made that the dispersive effects are regionally invariant.

A3. THE METHOD

To overcome the problems which effect intensity based ground motion estimates, a new technique is proposed for the estimation of acceleration attenuation functions for regions with inadequate strong ground motion data for the generation of empirical functions. This method incorporates a site intensity-acceleration correlation but on a much more restricted basis than previously used techniques. A limited amount of instrumental observations is required but in a form which can generally be obtained for regions of low seismic activity and short histories of instrumental coverage. The method is dependent on three assumptions.

The first, and least significant of the assumptions, is that some functional form exists which can depict the characteristics of peak acceleration attenuation in any region. The most commonly used function for acceleration attenuation equations is of the form:

$$\ln a_s = \alpha_1 + \alpha_2 M - \alpha_3 \ln (R + R_o) \tag{A6}$$

where a_s is the site peak acceleration, M is the magnitude of the causitative earthquake, R is the epicentral distance, R_o is a distance factor typically set to either zero or 25 km and α_1, α_2, α_3 are regression parameters based on observational data. In this report, only this form of attenuation function will be considered. The explicit form, however, is not critical to the method. It is assumed that this equation, given the appropriate regression parameters, will adequately characterize attenuation in any region. To obtain the regionally adjusted α_s for the area being studied, a data set used to evaluate these parameters is constructed on the basis of the other two assumptions.

The second assumption is that, at short epicentral distances, equal epicentral intensity earthquakes have equal levels of peak acceleration, regardless of regional source variations. Given a correlation between epicentral intensity and acceleration in some reference region, then this assumption implies that the relationship also holds in any other region. This is a restricted application of a site intensity-acceleration correlation in that only the more impulsive accelerations are assumed to correlate across regional boundaries. In this way the regionally dependent effects of distance on wavetrain dispersion are either eliminated or at least greatly reduced.

The use of epicentral intensity, as opposed to magnitude, as the basis for inter-regional comparison of near-field accelerations is significant. If magnitude were used then an implied assumption would be made that earthquake source characteristics, such as depth of occurrence, are regionally invariant. By using the surface effects, expressed as epicentral intensity, for comparison between regions and then converting intensity to magnitude using empirical relations, compensation for these source variations can be made.

A far-field acceleration estimate can be made by assuming that the peak acceleration at the radius of the felt area is a constant, or nearly so. The basis of the third assumption is that the minimum acceleration which can be perceived by a human is a function more of the human anatomy than geology, and thus should be regionally invariant. The radius of the felt area as a function of epicentral intensity can be obtained from historical, noninstrumental records. Again, empirical relations between epicentral intensity and magnitude permit the conversion of this information to a magnitude basis.

The question then arises as to what level of acceleration is appropriate at the limit of perceptibility. Experiments have been conducted which have found that the limit of perception of earthquake type motions is approximately 0.8 cm/sec^2 over the frequency range of 2 to 0.4 Hz (Ishimoto and Ootaka, 1933). The typical perception curve which was found is shown in Figure A2. As these experiments were conducted under laboratory conditions this value should be considered a lower bound. Field experiments conducted at the same time found a threshold value for earthquake perception of 1.7 cm/sec^2 (Inouye, 1933). Guttenberg and Richter (1956) report accelerations over the range of 1.6 to 3.0 cm/sec^2 for Modified Mercalli intensities of I and II in California. Based on the definitions of the intensity scale, the limit of the felt area should lie between these two intensities. The consistency of these values suggest that a reasonable value for use at the radius of the felt area should be between 1.7 and 4.0 cm/sec^2. The higher value would be more applicable in a region of low seismic activity where the association of slight vibrations with earthquakes might not be made as readily as in an active region.

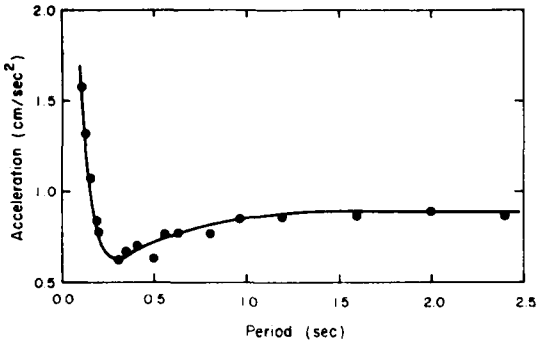

Figure A2. Minimum Perceivable Accelerations for Periods of Less Than 2.5 Seconds

Given these assumptions and an epicentral intensity-acceleration correlation for the reference region, a data set can be constructed for use in the regression of the α's of a regionally modified attenuation function. The data set would consist of a near-field acceleration estimate based on inter-regional correlation of epicentral intensity and a constant level of acceleration at the radius of the felt area which is a function of earthquake magnitudes. By constraining the distance factor, R_{ij}, in Eq. (A6), the evaluation of the constants of the attenuation function can be carried out by a simple least squared error fitting procedure.

The proposed method was used to generate attenuation functions for five subdivisions of the United States. These regions are shown in Figure A3 and are the same as those used by Brazee (1976) to develop the equations relating epicentral intensity and magnitude and radius of felt area which were used to generate the modified attenuation functions. The development of a relation for California was considered a partial test of the method. This application could only test the adequacy of the far-field assumption and of fitting the attenuation function to a limited data base. The near-field assumption could not be tested as the available epicentral intensity-acceleration correlations are based on California data. This, however, is not considered significant as all other procedures for obtaining acceleration estimates on the basis of site intensity make use of a more liberal form of this assumption.

Before proceeding with the application, two points should be discussed. The first concerns the distance at which the near-field estimate of acceleration is made. This evaluation can be made either at some fixed distance or at a distance which is a function of the event magnitude. The variable distance scheme could result in such large distances for large magnitude events that dispersion would become an important factor or, for small magnitude events, such small distances that any method of estimating acceleration would be invalid because of very near-field effects. Using the fixed distance requires only that the distance used be

significantly smaller than the radius of the felt area of the smallest magnitude used to develop the data set. In the following applications of the method, a distance of 15 km was used.

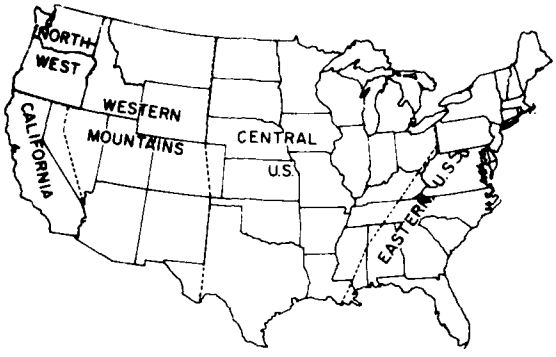

Figure A3. Regional Divisions Used in the Development of Derived Acceleration Attenuation Functions

Two methods are also available for the evaluation of the near-field accelerations. The first of these is to use a site intensity-acceleration correlation function of the form of Eq. (A5) or to convert epicentral intensity to equivalent magnitude in the reference region and to use a reference region attenuation function. In general, attenuation functions have lower standard errors than available site intensity relations, but the two methods are probably equal when the error of conversion from epicentral intensity to magnitude is included. The use of attenuation functions was selected for the following applications.

California - The basic equation for evaluating a California attenuation function is the function defining the radius of the felt area, R_f, in terms of event magnitude:

$$\ln R_f = 0.938 + 0.725\ M \ . \qquad (A7)$$

As the attenuation function used to evaluate the near-field accelerations is based on data from California, near-field accelerations can be determined directly on the basis of magnitude without the intermediate step of epicentral intensity comparison. Evaluation of the near-field accelerations were made using two different acceleration attenuation functions:

$$\ln a_s = 3.40 + 0.89\ M - 1.17 \ln R \qquad (A8)$$

and

$$\ln a_s = 6.16 + 0.65\ M - 1.30 \ln(R + 25) \qquad (A9)$$

both of which were developed by McGuire (1978 and 1974, respectively). Both 2.0 and 4.0 cm/sec^2 were used as the acceleration at the radius of the felt area. The smallest standard error of fitting were found using Eq. (A8) and 4.0 cm/sec^2.

The best fit equations, based on the standard errors of fitting, are given by

$$\ln a_s = 3.725 + 1.026\ M - 1.603\ \ln R \qquad (A10)$$

and

$$\ln a_s = 7.044 + 1.155\ M - 2.300 \ln(R + 25) \qquad (A11)$$

where R_o was set either to zero or 25 km. The curves generated from Eqs. (A8) through (A11) are plotted for the purposes of comparison in Figure A4 evaluated at 5.0 M and, at 7.0 M in Figure A5. The derived curves indicate a faster fall off of peak acceleration than either of the empirical functions. This becomes most apparent beyond 100 km. If the far-field assumption is correct, this difference can probably be explained by the fact that the empirical equations are based on data predominately from shorter epicentral distances.

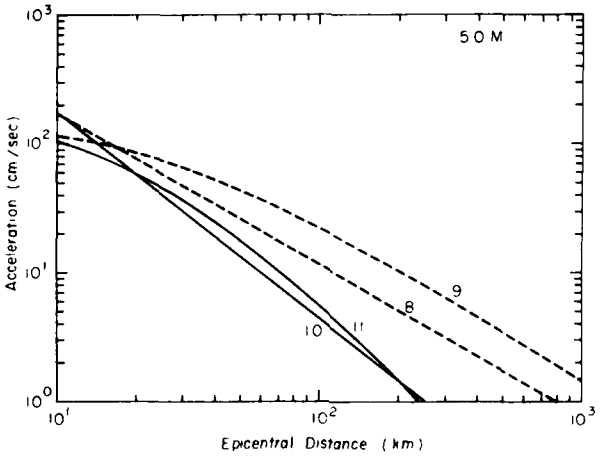

Figure A4. Derived (solid curves) and Empirical (dashed curves) Peak Acceleration Attenuation Functions for California Evaluated at 5.0 M. Numbers on curves refer to equation numbers given in text

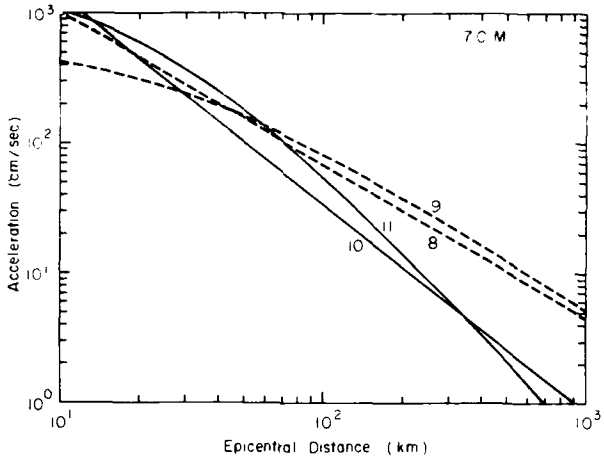

Figure A5. Derived (solid curves) and Empirical (dashed curves) Peak Acceleration Attenuation Functions for California Evaluated at 7.0 M. Numbers on curves refer to equation numbers given in text

In Figure A6, all four equations are evaluated at 6.55 M and plotted against sixty-one rock and stiff soil peak accelerations recorded during the Borrego Mountain (6.5 M) and San Fernando (6.6 M) Earthquakes (Seed et al, 1976). It is apparent the curves derived by the method proposed in this report do a better job of predicting the data beyond 100 km. The mean squared residuals of the natural logarithms of the data are 0.367, 0.587, 0.194, and 0.220 for Eqs. (A8), (A9), (A10), and (A11) respectively. Inside of 100 km the two sets of equations are essentially equal with mean squared residuals between 0.135 and 0.195. Outside of this distance a significant change occurs with mean squared residuals of 0.775, 1.269, 0.294, and 0.345, respectively.

Based on this test, it would appear that the method can produce a reasonable attenuation function for use over a wide range of distances. In addition, the success of the far-field assumption would suggest that it could be used as an additional restriction in the development of empirical functions if far-field data is lacking.

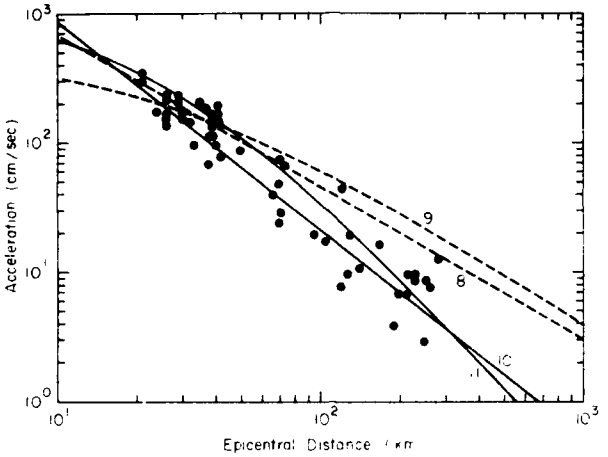

Figure A6. Derived (solid curves) and Empirical (dashed curves) Peak Acceleration Attenuation Functions for California Evaluated at 6.55 M, and Plotted Against Rock and Stiff Soil Accelerations Observed for the Borrego Mountain and San Fernando Earthquakes. Numbers on curves refer to equation numbers given in text

Other Regions - Attenuation functions were also developed for four other regions of the United States. The relationships used in the development of these functions and the resulting functions themselves are given in Table A1. The derived functions, including those generated for California, were evaluated for a magnitude of 6.0 M and plotted in Figure A7, for those with R_o set to 0 and in Figure A8 for those with R_o set to 25 km. At the present time virtually no data exists for the testing of these functions. The functions agree with the usually held concept that the attenuation throughout the western United States is fairly uniform and that attenuation is much lower in the Central United States with the Eastern United States being somewhere in between.

Finally, a comparison of the accelerations predicted for magnitude 4.0 M and 6.0 M earthquakes in the Central United States using the proposed method and site intensity based methods is shown in Figure A9. The site intensity methods shown in this figure use the intensity-acceleration and intensity and distance-acceleration correlations developed by McGuire (1977) in conjunction with intensity attenuation functions developed by Howell and Schultz (1975). While it is impossible at the present time to determine which of the equations is more realistic, it is apparent that significant differences exist between them.

Table A1. Derived Peak Acceleration Functions for Regions of the United States

Region	$M = a + bI_o$		$\ln R_f = c + dM$		$\ln a_s = \alpha_1 + \alpha_2 M - \alpha_3 \ln(R + R_o)$			
	a	b	c	d	α_1	α_2	α_3	R_o
California	2.149	0.487	0.938	0.725	3.725 7.044	1.026 1.155	1.603 2.300	0.0 25.0
Northwest	1.971	0.568	2.069	0.518	4.703 8.362	0.782 0.892	1.547 2.310	0.0 25.0
Western Mountains	1.226	0.704	1.994	0.515	5.021 8.758	0.706 0.812	1.548 2.327	0.0 25.0
Central United States	2.296	0.350	0.886	1.033	2.640 4.214	1.263 1.402	1.246 1.574	0.0 25.0
Eastern United States	-0.326	0.746	2.536	0.558	5.507 8.208	0.679 0.786	1.393 1.932	0.0 25.0

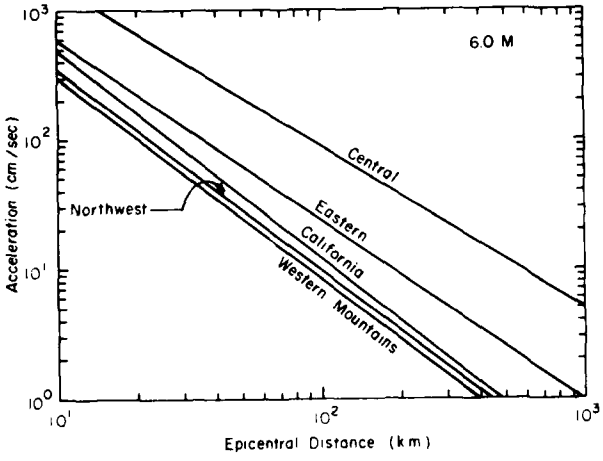

Figure A7. Derived Attenuation Curves, Using R_o Set to Zero, for the Five Subregions of the United States as Given in Table A1. All curves evaluated at 6.0 M

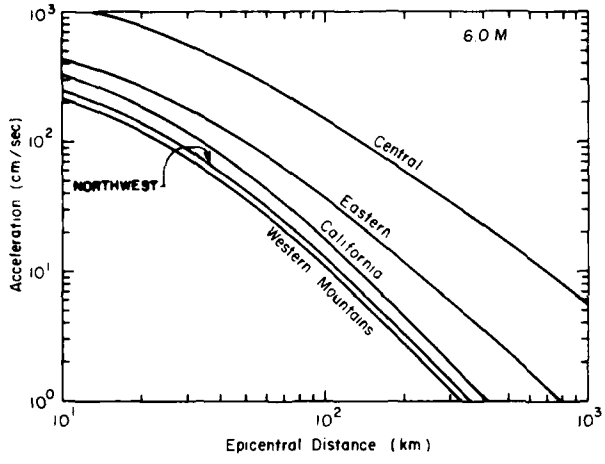

Figure A8. Derived Attenuation Curves, Using R_o Set to 25 km, for the Five Subregions of the United States as Given in Table A1. All curves evaluated at 6.0 M

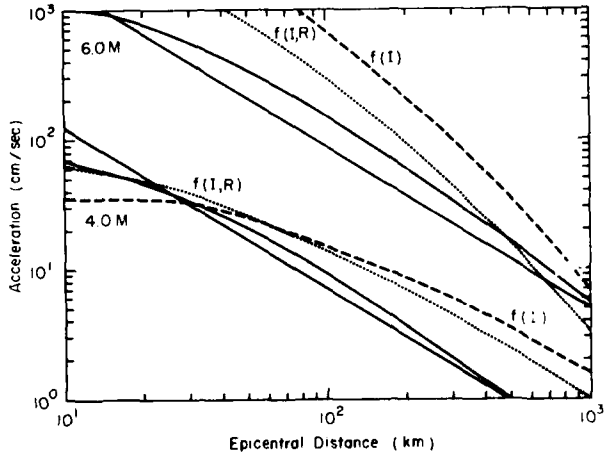

Figure A9. Derived Attenuation Curves and Site Intensity [f(I)] and Site Intensity and Distances [f(I, R)] Acceleration Attenuation Curves for the Central United States. Each type of curve is evaluated at 4.0 M and 6.0 M

A4. ERRORS

It is not possible to directly evaluate the errors associated with the attenuation functions derived using the method proposed in this report. One scheme which does seem reasonable, however, is to assume that the distribution of accelerations about the derived curves is similar to the distribution about the empirical curves for California. A standard deviation equal to those evaluated in California, or perhaps increased to be conservative, can be assigned to these functions. A typical standard deviation, based on the values listed by McGuire (1976) is about 0.707 for the natural logarithm of the peak acceleration and might be appropriate for use with the regionally modified attenuation functions.

A5. CONCLUSIONS

Although there are many significant problems associated with the use of strong ground motion attenuation functions, they do provide an important means for converting knowledge of seismic activity into estimates of engineering seismic risk. In this report a new method for the regional modification of peak acceleration attenuation functions has been presented and the method applied to derive attenuation functions for five regions in the United States. The method relies on two primary assumptions. First, in the near-field, the level of acceleration causing a given epicentral intensity is regionally invariant. Second, that the level of acceleration at the radius of the felt area is a constant. Available data tends to support the second assumption while the first is a restricted application of the assumption used in previously suggested methods.

The application of this technique to the development of an attenuation function for California indicates the feasibility of the approach. The derived functions predict peak accelerations for the Borrego Mountain and San Fernando Earthquakes at least as well as the two empirical equations to which they were compared. Beyond 100 km, the derived functions were found to be significantly more accurate than the empirical functions.

Peak acceleration attenuation functions were also generated for four other regions of the United States. While the errors associated with these functions can not be directly calculated, it is suggested that the errors might be similar to those found for empirical functions. One advantage of the proposed method is that, as observational data becomes available in the region for which the modification is conducted, it can be incorporated into the data base used for regression of the attenuation function parameters, thus providing an improving estimate of the regional attenuation function until the point is reached where the observational data alone is sufficient.

Appendix A References

Brazee, R.J. (1976) Analysis of Earthquake Intensities With Respect to Attenuation, Magnitude and Rate of Recurrence, Natl. Oceanic Atmospheric Admin. Technol. Memo. EDS-NGSDC-2.

Esteva, L. (1970) Seismic risk and seismic design decisions in Seismic Design for Nuclear Power Plants, R. Hansen, Editor, MIT Press, Cambridge, Massachusetts, pp 142-182.

Gutenberg, B., and Richter, C.F. (1942) Earthquake magnitude, intensity, energy, and acceleration, Bull. Seism. Soc. Am. 32:163-191.

Gutenberg, B., and Richter, C.F. (1956) Earthquake magnitude, intensity, energy, and acceleration, Bull. Seism. Soc. Am. 46:105-145.

Howell, G.F., and Schultz, T.R. (1975) Attenuation of Modified Mercalli intensity with distance from the epicenter, Bull. Seism. Soc. Am. 65:651-666.

Inouye, W. (1933) Observations of near earthquakes on Mt. Tubuka, Bull. Earthq. Res. Inst. 11:69-81.

Ishimoto, M., and Ootuka, M. (1933) Determination de la limite perceptable des secousses, Bull. Earthq. Res. Inst. 11:113-121.

McGuire, R.K. (1974) Seismic Structural Response Analysis Incorporating Peak Response Regressions on Earthquake Magnitude and Distance, M.I.T. Dept. of Civil Eng. Research Report R74-51.

McGuire, R.K. (1976) FORTRAN Computer Program for Seismic Risk Analysis, U.S. Geol. Surv. Open File Report 76-67.

McGuire, R.K. (1977) The use of intensity data in seismic hazard analysis, Proc. Sixth World Conf. on Earthq. Eng., New Delhi, India, pp 709-714.

McGuire, R.K. (1977) Seismic ground motion parameter relations, The Use of Probabilities in Earthquake Engineering, ASCE Fall Meeting Convention and Exhibit, Preprint 2913, San Francisco, California.

Murphy, J.R., and O'Brien, L.J. (1977) The correlation of peak ground acceleration amplitude with seismic intensity and other physical parameters, Bull. Seism. Soc. Am. 67:877-915.

Seed, H.B., Murarka, R., Lysmer, J., and Idriss, I.M. (1976) Relationships of maximum acceleration, maximum velocity, distance from the source, and local site conditions for moderately strong earthquakes, Bull. Seism. Soc. Am. 66:1323-1342.

Trifunac, M.D., and Brady, A.G. (1975) On the correlation of seismic intensity scales with peaks of recorded strong ground motion, Bull. Seism. Soc. Am. 65:139-162.

Printed by
United States Air Force
Hanscom AFB, Mass. 01731

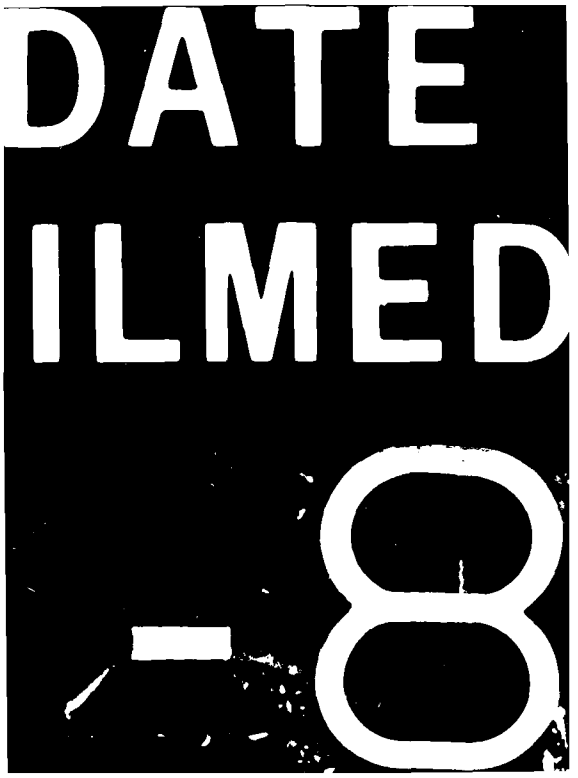
DATE
ILMED
-8